X-645-72-293

PREPRINT

NASA TM X-66035

LATITUDE AND LOCAL TIME DEPENDENCE OF PRECIPITATED LOW ENERGY ELECTRONS AT HIGH LATITUDES

GEORG GUSTAFSSON

AUGUST 1972

GSFC

GODDARD SPACE FLIGHT CENTER

GREENBELT, MARYLAND

LATITUDE AND LOCAL TIME DEPENDENCE OF PRECIPITATED LOW ENERGY ELECTRONS AT HIGH LATITUDES

by

Georg Gustafsson*
NASA Goddard Space Flight Center
Greenbelt, Maryland 20771

August 1972

*On leave from Kiruna Geophysical Observatory, S-981 01 Kiruna, Sweden

I

Abstract

Data from particle detectors on board the satellite OGO-4 were used to study the precipitation of electrons in the energy range 0.7-24 keV. The latitude dependence of these particles in the local time region from midnight to dawn has been investigated in detail.

The analysis shows that the precipitation of particles of energies 2.3-24 keV is centered at an invariant latitude of about 68° at midnight with a clear shift in latitude with increasing local time and this shift is more pronounced for lower energies. The highest fluxes of particles in this energy interval are measured at midnight and they decrease rapidly with local time. In the dawn region the location of the maximum precipitation for different energies varies about 1° of latitude for each unit of Kp, but the relative distribution remains almost unchanged. The fact that different energies have their maxima at different latitudes implies that the flux spectrum of precipitated particles, when measured at a certain latitude, has a peak at an energy corresponding to the energy of maximum precipitation at that latitude.

The data in the energy range 2.3-24 keV supports a theory where particles are injected in the midnight region from the tail gaining energy due to a betatron process and then drift eastwards in a combined electric and magnetic field.

The main part of the electrons at 0.7 keV show a different behavior than those at higher energies. They seem to undergo an acceleration process which is rather local, sometimes giving field aligned fluxes which may be superimposed on the background precipitation. The structural precipitation of 0.7 keV electrons has been found to coincide on a statistical basis with the region of structural aurora indicating a relationship between the two phenomena.

1. Introduction

The understanding of the dynamical behavior of different particle populations in the magnetosphere and their relations to phenomena in the polar ionosphere is far from complete. For recent reviews on the subject see Hoffman (1972), Hultqvist (1972) and Paulikas (1971). The purpose of this study is to present some additional information on the morphology of electron precipitation in the polar regions, particularly on the dawn side and to relate this to sources of particles further out from the earth.

Measurements by electron detectors on board the polar orbiting satellite OGO-4 have been used in this study. Four of the detectors were always pointed radially away from the earth (0°) and measured electrons in energy bands (about 15%) around 0.7, 2.3, 7.3 and 24 keV. Three others were positioned 30°, 60° and 90° to the earth-spacecraft radius vector, and centered at 2.3 keV. The height of the satellite varied between 400-900 km. The sampling of the 0° detectors was made simultaneously for all the energies and the storage time was 135 msec. or shorter. For further details of the experiment see Hoffman and Evans (1967).

The analysis has been based on two types of raw data, one in which the full time resolution of the instrument has been used and one where the intensity of each energy channel has been averaged over one degree of invariant latitude.

The one-degree data has been used to locate the latitude of the maximum of precipitation for each energy channel, and the locus of these maxima has been studied as a function of local magnetic dipole time (MLT).

The selection of the data has been made as follows. The passes have been included if the 7.3 keV counting rate was greater than 10 counts per readout (corresponding to 74 counts/sec or more) and there was only one major

maximum in the latitude range 65-78° invariant latitude at 7.3 keV. This means that about 35% of the passes have been excluded due to low intensity and 23% have been rejected due to their complexity. The features which will be demonstrated apply to the remaining 42% of the data. The magnetic activity for the events was usually in the range of 2-3 of Kp. The study has also been limited to the time interval 2200-1040 MLT.

The counting rate of the 24 keV detector was in general rather low and the 2.3 keV channel had a relatively high background noise which means that the accuracy of the 0.7 keV and the 7.3 keV channels was higher than in the other channels. Therefore the relation between 0.7 and 7.3 keV will be mostly used in the discussion.

In the next sections of this paper we will describe the locus of maximum precipitation as a function of invariant latitude and magnetic local time and its relation to the auroral oval and dependence on magnetic activity. After this we will discuss the average 4-point differential flux spectra as a function of local time and latitude. The locus of the maximum precipitation is then transformed to the equatorial plane in the outer magnetosphere. With the assumption that the particles are injected at midnight and drift eastward, we are able to consider the necessary electric fields for this morphology. In Section 7 the spectra at satellite altitude will be compared with the spectra measured by the Vela satellites in the tail. Finally we conclude these descriptions by a discussion of the 0.7 keV precipitation structure as this energy channel shows a structure which is different from the other channels at all local times.

2. Location of maximum precipitation as a function of local time and latitude

In this section the the one-degree invariant latitude averaged data has been used. The location of the maximum for each energy channel and satellite pass has been read from the data together with the local time. This is plotted in Figures 1a-d.

In the midnight region up to 0200 MLT all the energy channels show a maximum which is located on the average at 67-69° invariant latitude. For individual passes higher energies have a tendency to be precipitated at lower latitudes than the lower energy channels.

Later in the morning the spread in latitude of the maximum precipitation for different energies is more pronounced (see Figures 1a-d). The lines in the figures represent a least square fit. For later local times there is also a trend towards higher latitude. A comparison between the average lines for the different energies has been made in Figure 2 (the magnetic contours in the figure will be discussed later). In particular, it has been noted that in no pass was the maximum of the higher energy channel located at a higher latitude than the lower channel beyond 0400 MLT. This is demonstrated in Figure 3 which shows the maxima when each 7.3 keV maximum has been normalized to their average location (represented by the line in the figure) and a corresponding latitude difference has been added to the location in latitude of the maxima of the other energies. The scattering of the points in Figure 3 is much less than in Figure 1 which indicates that a large part of the scattering in Figure 1 is due to variation in the magnetic activity between the events. Looking more carefully on Figure 1 it can be seen that there is a tendency in all the energy channels for a cosine dependence on local time; e. g., at 10 MLT the median values are at lower latitudes than

the average line. This variation of location in latitude with local time is similar to the location of the equatorward border of the auroral oval.

3. Location of maximum precipitation and the auroral oval

Starkov (1969) has shown that the location of the equatorward boundary of the auroral oval varied with local time as

$$L = 90 - 18 - 0.9Q - 5.1 \cos (t - 12^{o})$$

where L is the location in invariant latitude Q is the magnetic Q-index and t is the local magnetic time measured in degrees. With Q = 3 it is found that the oval boundary is about 2° equatorward of the precipitation maximum of 7.3 keV at 0400 MLT and crosses the average location of 7.3 keV at 0800 MLT, indicating that the average energy of the electrons precipitated in the oval decreases with local time. However, if the maximum of the auroral oval for Q = 3 as given by Feldstein and Starkov (1967) is compared with the location of maximum precipitation of Figure 2 it is found that the oval maximum coincides with the location of 2.3 keV electrons at both 0400 MLT and 0800 MLT (the two times shown by the authors). But as the maxima of different energy channels are very close in latitude at 0400 MLT as seen from Figure 2 (only 0.5 degrees between 2.3 and 7.3 keV) and the location is strongly dependent on magnetic activity this result may not be significant.

A more striking difference between the oval and the location of precipitation maxima is that the width of the oval is decreasing with local time while the locus of the maxima at different energies become more separated with local time. The width of the precipitation profile (when measured at half intensity level) of each energy channel when crossing the auroral region is also increasing with local time. For example, the 7.3 keV profile defined as

the width in latitude degrees at half intensity level was on the average 2.0°, 2.3°, 2.9° and 3.4° for the local time intervals less than 0200 MLT, 0200-0400 MLT, 0400-0600 MLT and greater than 0600 MLT, respectively. But the profiles measured above a fixed threshold decrease considerably with local time due to the decrease in the total flux. The 0.7 keV channel is different from the other energies because the profile is not smooth. Usually several maxima appear even when one-degree averages in latitude are used which makes it difficult to measure the width. It will also be shown later that the shape of the particle spectrum is roughly constant with local time for energies 2.3 keV and higher. It is known that the energy range of the particle spectrum causing the main part of the visible aurora around midnight is rather narrow and centered around 5 keV (see Gustafsson, 1970). Therefore, a suitable decrease in the average energy of the particle spectrum with local time together with a flux threshold which matches the auroral oval at midnight will give a precipitation pattern which resembles that of the auroral oval. The conclusion that the visible aurora on the dayside is caused mainly by particles of an energy less than 2.3 keV is in accordance with the measurements of the height of the aurora in that area by Starkov (1968). He found heights varying between 145-175 km. The results above also conform with the spectral measurements of the aurora by Eather and Mende (1972).

The dependence of the location of maximum precipitation on magnetic activity is very pronounced. As was mentioned earlier the scattering of points in Figure 1 is much larger than that in Figure 3 and this is attributed mainly to the effects of magnetic activity. A comparison between the location of the precipitation maximum of 7.3 keV and the level of Kp for the time interval 0440-0800 MLT is shown in Figure 4. The Kp classes 0 and 4 are averages of less than 10 events and are rather uncertain. The equation of

the line in Figure 4 is $\Delta lat = -0.95\ Kp + 2.6$ where Δlat is the location of the 7.3 keV precipitation relative to the average location line in Figure 1c. The relation shows that the average Kp for the events included was 3- and that the locus was shifted 0.95^{o} in latitude towards the equator for each unit of Kp. The reason for choosing the 0440-0800 MLT interval was that Kp was most evenly distributed there. However, similar results were obtained closer to midnight. A corresponding comparison for the other energy channels have not shown any significantly different result. More detailed studies on the dependence on magnetic activity have been made by Riedler and Borg (1971) and Burch (1972).

These results are in good agreement with the dependence of the auroral oval on magnetic activity. As mentioned earlier Starkov (1969) has found a dependence of 0.9^{o} for each unit of Q for the southern border.

4. The distribution of the flux of precipitated electrons as a function of local magnetic time and latitude

The maximum flux of precipitated electrons for each energy channel and satellite pass has been averaged over three different intervals of time 2230-0200, 0200-0520 and 0520-0800 MLT. This means that the points in the spectra are usually from different latitudes for the different energy channels (it might be considered as an envelope spectrum). The result has been displayed in Figure 5. In the 24, 7.3 and 2.3 keV channels the flux is decreasing from midnight to dawn but at 0.7 keV the flux at 0520-0800 MLT is higher than the flux at 0200-0520 MLT. This indicates that there is an additional source of electrons at local times beyond 0520 MLT for the lowest energy.

The 0.7 keV channel shows in general very large peaks particularly in the dawn to noon region when looking at high time resolution recordings.

Therefore, it might be expected that excluding the peaks and only measuring the background would lower the influence of the dayside source. The result of this high time resolution study has been included in Figure 5 (called "minimum 0.7 keV level"). However, the relation between fluxes at different local times still remains approximately the same as before. The reason seems to be that the peaks at 0.7 keV on the dayside are so large and frequent that they contribute to the minimum 0.7 keV level. If the 0.7 keV flux is measured at the latitude where the 7.3 keV channel has its maximum, the 0.7 flux decreases at all local times like the other channels. This will be further discussed later. It may also be noted that even with the minimum level of 0.7 keV the flux at 0.7 keV is at least a factor of 5 higher than the 2.3 keV flux. This is of significance when comparison with the spectrum in the tail is made later.

The energy flux spectra may be obtained by converting the flux spectra described above (see Figure 6). The energy flux is almost constant from 2.3 to 7.3 keV for the three local time intervals but varies a factor 2 to 4 between 0.7 and 2.3 keV. In this case the minimum 0.7 keV level gives an energy flux which is comparable to the 2.3 keV flux except for the 0520-0800 MLT region. Integrating the energy flux from 0.7 to 24 keV gives 2, 0.8 and 0.6 ergs cm^{-2} sec^{-1} sr^{-1} for the time intervals 2230-0200, 0200-0520 and 0520-0800, respectively.

A set of spectra of electrons as a function of latitude has been obtained by using the whole profile over the precipitation region of a satellite pass. A typical example has been shown in Figure 7. This pass which was at 0600 MLT shows clearly the displacement in latitude of flux maxima for the different energies. The maxima are at 66-67, 69-70 and 70-71

degrees of latitude for 24, 7.3, 2.3 and 0.7 keV respectively. It also shows that the flux of electrons at 7.3 keV was higher than at 2.3 keV below an invariant latitude of 68°. Looking through all the events used in this study it has been found that the ratio 7.3 to 2.3 keV rarely exceeds three but is frequently greater than one.

It may be noticed in Figure 7 that below 67.5° latitude the ratio of 0.7 to 7.3 keV fluxes increased towards the equator, a phenomenon which is observed quite often.

5. Distribution of particles in the equatorial plane deduced from the precipitation maxima in the ionosphere

It has been shown by DeForest and McIlwain (1971) that electrons in the energy range considered here are generally injected close to midnight and then drift eastward in longitude. Their measurements were carried out at ATS at 6.6 R_e and should be applicable here at least for the higher energies. This view is supported in this study for the 2.3, 7.3 and 24 keV channels which show a decrease in flux with local time. As the pitch angle distribution of the particles drifting in the equatorial plane is not known, it will be assumed here that they have a pitch angle of 90° and that a pitch angle diffusion mechanism causes the precipitation. This assumption is supported by the fact that the maximum precipitation at 2.3 keV has been found to be at the same latitude for 0° and 90° angle (relative to the Z-axis) at all local times and the width of the precipitation profiles in latitude is not widening appreciably with local time for any energy channel. According to the calculations by Roederer (1967), as an example, it might be expected that particles with a pitch angle of 50° at the equator at midnight should show a shell splitting of 2° in latitude beyond 1000 MLT. If these particles were precipitated (with sufficiently strong pitch angle scattering), they could be detected in the data. This implies that the particles

have a range of pitch angles which is likely to be centered around 90° during most of the time while drifting in longitude. The velocity of electrons drifting from the midnight region with a pitch angle of 90° in a combined electric field $\underset{\sim}{E} = -\nabla\phi$ and a magnetic field $\underset{\sim}{B}$ is given by

$$\underset{\sim}{V}_D = \frac{\underset{\sim}{B} \times \nabla (\underset{\sim}{\mu} \cdot \underset{\sim}{B} + q\phi)}{q B^2}$$

where $\underset{\sim}{\mu}$ is the magnetic moment and q is the charge of an electron. The electrons will drift along a path where the total energy $W = \underset{\sim}{\mu} \cdot \underset{\sim}{B} + q\phi$ is constant.

The contours of constant magnetic field at the equator as given by Fairfield (1968) are projected along the magnetic field lines down to the altitude of the OGO-4 observations, (using Fairfield's model), where they are compared with the location of the precipitation maxima. It is found, as shown in Figure 2, that the maxima of the energies 7.3 and 24 keV follow lines of constant magnetic contours in the equatorial plane very closely. For 2.3 and 0.7 keV there is some deviation. In Figure 2 the locus of the maxima have not been drawn from midnight up to 0400 MLT because they have to be measured with the accuracy of a fraction of a degree in order to make a comparison with the magnetic contours. However, the relative locations of the maxima of the energy channels (cf. Figure 3) around midnight indicate that the above statement that the maxima follow constant magnetic contours from midnight is valid in most cases.

The fact that the 24 keV and 7.3 keV particles are located along constant magnetic contours shows that these particles are very little influenced by the electric field or the field has to be perpendicular to the magnetic contours.

There is also the possibility that the precipitation mechanism determines the location but that seems less likely as it requires a complicated electric field pattern and a very energy sensitive precipitation mechanism.

The drift motion of the 0.7 keV electrons is almost completely determined by the electric field because the magnetic gradient drift corresponds to only a fraction of a mV/m of electric field which is less than what has been measured (cf. Heppner, 1972). But even in this case the particles are found along approximately constant magnetic contours except on the dayside close to the magnetopause. As was mentioned earlier the flux of 0.7 keV electrons does increase when approaching dayside, which makes it unlikely that these particles are drifting from the nightside. At least it may not be considered as the main source. The details of the 0.7 keV precipitation will be farther discussed in a later section.

6. An estimate of the electric field

Making the assumption that the particles are injected at geomagnetic midnight, and that they cause a magnetic bay as observed on the ground, the delay between the appearance of the bay and the precipitation of particles at a certain time in the morning hours is then a measure of the drift speed of the particles. However, it has proved to be difficult to find isolated bays related to the precipitation. The cases which have been found are displayed in Figure 8. A bar has been drawn corresponding to the beginning and the end of the bay. The thickness of the bar is related to the intensity of the 2.3 keV precipitation. A thick bar is therefore likely to correspond to the center of the bay and hence the center of the bar gives the most likely delay time measured after the bay. Particular care has been made to determine the end of the bays (as this will correspond to shortest delay or maximum electric

field). In the cases which have been shown the magnetic activity was less than 20γ at all the magnetic stations available from the midnight region from the end of the bay to the time of the satellite pass. For the cases which have been shown an upper limit of the equatorial electric field of 0.25 mV/m has been obtained. However, it should be pointed out that this applies to a few clean magnetic events and may well be larger on the average. It has also been determined from precipitated particles and therefore dependent on the efficiency of the precipitation mechanism.

It has also been found that in all the satellite passes where there is an appreciable enhancement of 7.3 keV (above the background level) there is always an increase of 2.3 and 0.7 keV flux. That is not always the case for 24 keV but that may be a threshold effect as the countrate of that detector is on the average rather low compared with the other channels. This indicates an electric field of about 0.4 mV/m as this is approximately what is needed to get the same drift velocities for 0.7, 2.3 and 7.0 keV electrons.

7. A comparison between particle spectra in the tail and the ionosphere

Evidence has been given among others by Frank (1962), Pfitzer and Winckler (1969), Arnoldy and Chan (1969), Chase (1969) and Lezniak and Winckler (1970) that electrons from the tail are injected into the magnetosphere in the midnight region. From the data shown here this injection seems to be down to 7-8 R_e around midnight.

From Liouville's theorem the density of particles in phase space f is constant along the particle's trajectory. The density is related to the differential flux j (see Nakada et al., 1965) by

$$f(E,\alpha) = \frac{1}{2mE}\, j\,(E,\alpha)$$

where m is the mass, E the energy and α the pitch angle of the electron. Assuming that the first adiabatic invariant is conserved and considering only 90° particles $\frac{E_1}{B}$, where B is the magnetic field strength, is constant. Equating the density in the tail (1) to the density in the magnetosphere (2) we get

$$j\ (\frac{E_1}{E_1}) = j\ (\frac{E_2}{E_2})$$

and with $E_1/E_2 = B_1/B_2$

$$j\ (E_1) = \frac{j\ (E_1 \cdot B_2/B_1)}{B_2/B_1}$$

Taking the field in the tail equal to 20γ (cf. Fairfield, 1968) and projecting the measured spectrum of Figure 5 for the midnight region out to the equatorial plane, the spectrum in the tail has been calculated from the above formula. The estimated spectrum has been shown in Figure 9 together with some spectra measured by Hones et al, (1971). The similarity between the estimated and measured spectra in the tail is striking for the three points corresponding to 2.3, 7.3 and 24 keV in the ionosphere, but the 0.7 keV point is an order of magnitude too large when compared with the disturbed conditions in the tail. It is in fact close to the flux found at Vela during quiet conditions.

It was mentioned earlier that if the minimum level of 0.7 keV is considered (cf. Figure 5) the flux is a factor 7 lower but the flux at 0.7 keV would still be higher than at 2.3 keV. This means that the decrease in the flux which has been found at Vela below 0.5 keV in the tail can not be estimated from the spectrum at satellite altitude close to the ionosphere.

Therefore, this rather crude comparison of the spectra in the tail and the ionosphere suggests that there is some additional mechanism causing the high flux at 0.7 keV which is observed.

8. The structure of the 0.7 keV precipitation

The precipitation in the 0.7 keV channel has a different structure than the other energy channels at all local times considered here, 22 - 10 MLT. In the time sector 0400-1000 MLT the general pattern of a recording of a satellite pass over the precipitation region shows a rather smooth equatorward part in all the four energy channels and a poleward region with peaks of a few sec. or a few tens of km at 0.7 keV with magnitudes 10 or more times greater than those in the smooth region. The frequency of occurrence of the 0.7 keV peaks as a function of local time and invariant latitude has been studied by Hoffman and Berko (1971). But they have not included the peaks superimposed on the smooth region around midnight. The 0.7 keV peaks have also been classified as bursts by Hoffman and Evans (1968). In this time sector the 0.7 keV peaks in the smooth region are rarely higher than a factor of two relative to the smooth background. Only in one pass out of ten has such a peak been found. The transition between the two regions (the smooth and the burst region) is sometimes only a fraction of a degree in latitude. The bursts reach usually up to 78-80° in invariant latitude and sometimes even higher. Two passes in this time sector have been shown in Figure 10. Orbit 276 shows a 2.3 keV precipitation region somewhat wider than average, the shift in latitude of the different maxima for the different energies, and that the 0.7 keV bursts are larger than in the smooth region even when averaged over 1° in latitude. The transition region is not very sharp. Orbit 3216 shows a very pronounced shift in latitude with energy. The width of the smooth region is rather typical. This pass was at about 0600 MLT and the average of the bursts

here is less than in the smooth region and the bursts extend only up to a latitude of 76°. The transition between smooth and burst regions is very sharp, with the 7.3 and 2.3 keV fluxes changing more than an order of magnitude in 0.7 sec. A good correlation exists between 0.7 and 7.3 keV precipitation in the bursts when the flux is high enough to give a measureable flux at 7.3 keV. The ratio between the 0.7 and 7.3 keV fluxes is on the average 24 in the smooth region and 920 in the bursts for this time sector.

In the midnight sector the smooth region is not as evident as later in the morning, because it shows usually a rather peaked structure. The situation can be described as 0.7 keV bursts (the peaks are frequently a factor of 10 above the background) superimposed on the smooth region. In about half the number of passes a clean burst region can be identified poleward of the main precipitation of 7.3 keV and it generally covers the latitudes 67-72°. Two examples of night passes have been shown in Figure 11. Pass 888 is an example where the 0.7 keV bursts are superimposed on the smooth region. For example, it can be seen that the peak at about 69° invariant latitude has a ratio in the excess flux above the smooth background which is about 300 for 0.7 keV/7.3 keV, while the ratio between the backgrounds in the two energies is 16. This may be compared with the average ratio in the midnight sector which is 12 in the smooth region and 360 in the 0.7 keV burst region. The fact that the peaks above the background of the smooth region show the same ratio of 0.7 keV to 7.3 keV is the reason for stating that the 0.7 keV bursts are superimposed on the smooth region. Pass 888 also shows that there is a southern border below which there is no burst: e.g., 66.4° in this case. It may also be pointed out that similar peaks in the precipitation have been shown to be related to visible auroral forms by Gustafsson (1970) and that the peaks in these cases are related to spatial

structures with large east-west extent rather than time variations. Pass 2606 is a case where the smooth and the burst regions are clearly separated.

The location of the burst regions varies with local time as shown in Figure 12 where the burst region has been defined as the region of 0.7 keV bursts poleward of the smooth 7.3 keV precipitation. This means that bursts can be found much further south in the midnight region. The line drawn in Figure 12 represents an auroral orientation curve by Gustafsson et al., (1969). The auroral orientation curves represent the east-west alignment of auroral arcs on a statistical basis. It can be seen that the auroral orientation curve crossing the midnight meridian at 68° does not follow any of the precipitation channels but rather seems to be centered in the region of peaked 0.7 keV precipitation in the local time interval 00-10 MLT.

The amplitude of the 0.7 keV bursts have a significant minimum at 0200-0400 MLT. The amplitude of the largest peak of 0.7 keV during each pass has been plotted in Figure 13. It may be noted that the decrease in magnitude of the 0.7 keV bursts by a factor of 2.3 from midnight to 0400 MLT is similar to the decrease in the other energies over the same time interval, and that the increase in the 0.7 keV channel for later MLT is not reflected in the other channels. The ratio 0.7 to 7.3 keV flux increases with local time;it is 360, 400, 590, 820 and 920 for the local magnetic times 00, 02, 04, 06 and 08 respectively.

It was mentioned earlier that the flux of 0.7 keV electrons increased from 04 MLT to 08 MLT even if the "minimum level" of the 0.7 keV channel was considered. However, if the flux of 0.7 keV is measured at the same latitude as the 7.3 keV maximum a decrease with local time similar to the other channels is found even in this local time interval.

To summarize this section the 0.7 keV precipitation can be described as consisting of three categories. One, which resembles the higher energy

channels, has a general smooth precipitation maximum over a few degrees in latitude and the flux decreases with local time: the ratio 0.7 to 7.3 keV flux is less than 15. The second type consists of narrow peaks which could be either temporal or spatial. There are some indications that at least those at midnight are spatial. Usually they are located on the poleward side of the 7.3 keV smooth region but may at times be superimposed on it around midnight. The amplitude of the bursts decrease with local time and the ratio 0.7 to 7.3 keV is about 400. Finally the third type consists of bursts mainly in the 06 - 10 MLT region (here studied up to 10 MLT but has been found by Hoffman and Berko, 1971, to extend over the entire dayside region). The flux of the bursts when averaged over one degree in latitude dominates over the background flux in the smooth region. This means that the one degree average data mainly reflects the smooth precipitation in the midnight to 06 MLT interval and the burst precipitation later in the morning. The magnitude of the bursts increases with local time and the ratio 0.7 to 7.3 keV flux is of the order of 1000. The location of the bursts is generally separated and to the poleward side of the smooth 7.3 keV precipitation region. Passes have been found where there is a smooth region but no bursts beyond 06 MLT but these are rare exceptions.

9. Discussion

An analysis of the distribution of precipitated electrons in latitude and local time, has shown that the main part of the fluxes in the 2.3, 7.3 and 24 keV channels have the same characteristics. They show a relatively smooth region of precipitation (when looking at a logarithmic record) which is centered at 68° invariant latitude at midnight and at higher latitudes in the morning hours. There is also a clear shift in latitude for different energies:

e.g., at 1000 MLT the energies 24, 7.3 and 2.3 keV are centered at 71.3°, 72.2° and 73.7° respectively. This shift is difficult to establish in the midnight region but there are indications that the different energies are shifted in a similar fashion as for later local times. It has also been demonstrated that the relative location of the precipitation maxima in the different channels is unchanged when the magnetic activity changes but the absolute location varies about one degree in latitude for each value of Kp.

It has been shown by DeForest and McIlwain (1971) at 6.6 R_e in the equatorial plane that the particles in these energies drift from the midnight region eastward. As this is very close to the precipitation maximum around midnight and there is no particular change in the character of the precipitation in these latitudes it is likely that the particles discussed here belong to the same category and drift from midnight towards dawn. This is also supported by the fact that the flux decreases with local time.

It has also been possible to relate the precipitation in the morning hours to magnetic bays around midnight in a few cases. A comparison with the particle spectrum in the tail has shown that the tail is a likely particle source for the precipitation. However, it seems to be necessary that the particles drift most of the time at about 90° pitch angle because no "shell splitting" has been observed. An electric field with a magnitude of a few tenths of one mV/m in the equatorial plane, which is directed approximately perpendicular to the magnetic contours, is required to explain the observations. This is consistent with extrapolation of low altitude measurements (Heppner, 1972).

From rocket experiments it has often been reported that there is a maximum in the differential number flux spectrum above a few keV. That has been found to be the general case here for the latitude where 7.4 keV has its maximum.

The flux at 7.3 keV when compared with 2.3 keV, measured at the same latitude, is 2 to 3 times larger. But the 7.3 keV, and 2.3 keV flux each measured at the latitude where they have their maximum when crossing the precipitation region shows that 7.3 keV is usually less than the 2.3 keV flux. In particular, dawn region cases may be found where the precipitation profile is narrow in latitude and well separated from the other energy channels giving an almost monoenergetic "point" spectrum.

The 0.7 keV precipitation has been found to be much more complex than that of the other channels. There is in general a smooth region at all local times which shows the same characteristics as the other channels.

The most striking feature of the 0.7 keV channel is that peaks occur which are one to two orders of magnitude above the background. Often they are quite isolated, but generally correlated with peaks at 7.3 keV with flux ratios varying between 350 - 1000. The smooth region often shows a sharp poleward termination and the 0.7 keV peaks are observed beyond that termination but in the midnight region the peaks are sometimes superimposed on the smooth region. The amplitude of the peaks has a minimum at 02-04 MLT which might indicate that the midnight peaks have a different source than the day peaks. It may also be pointed out that anisotropies at 2.3 keV electrons reported by Berko (1972) have a maximum occurrence at midnight and at 70-72^{o} in invariant latitude and decrease towards dawn with very few cases found on the dayside, while anisotropies at 1.3 keV reported by Holmgren and Aparicio (1972) show a second maximum in the day. This indicates also that there are two different kinds of particle populations at these low energies in the latitude range where the 0.7 keV peaks are observed.

A comparison has been made between the auroral oval and the precipitation in the 0.7 to 24 keV range. It seems difficult to relate the oval to the

precipitation because the oval has a large extension around midnight but is rather narrow on the day side, which is the opposite to what the 24, 7.3 and 2.3 keV profiles show (when measured at half intensity level). It is also known that the main auroral features are caused by electrons of an energy of about 5 keV on the night side. Gustafsson (1970) demonstrated a number of examples where peaks in the spectra at 6.3 keV were very closely related to the aurora as measured on the ground. It has been found here that the ratio 2.3 to 7.3 keV is relatively constant with local time (when measured at maximum precipitation) which means that the auroral oval (related to the flux of electrons above a constant threshold with local time) can be explained by decreasing the average energy, and the flux of ~5 keV electrons with local time. If the peaks of 0.7 keV in the midnight sector are considered as superpositions on the smooth region the auroral oval is found to be contained within the region of peaked 0.7 keV precipitation at all local times. As mentioned earlier, peaks in the midnight sector are related to auroral arcs. It is also well known that auroral arcs on the day side have different characteristics. Up to about 80° invariant latitude, they are east-west aligned but have a much shorter duration and lower intensity that at night. Comparing the auroral orientation curves (cf. Gustafsson et al., 1969) with the locus of the maximum precipitation, it is found that they deviate strongly for all the energy channels. In fact, they appear to follow the general location of the 0.7 keV peak locations as a function of local time. In Figure 12 it can be seen that the burst region is in general poleward of 74° at about 10 MLT and the auroral oval by Feldstein and Starkov (1967) is located at 74-76 at Q = 3. Qualitatively, therefore, the auroral arcs are located in the region of peaked precipitation of 0.7 keV at all local times

from midnight to 10 MLT and the characteristics of the arcs may be related to the spectral structure of the peaks. The detailed relation between the peaked precipitation and the extended east-west forms of the aurora (which is the auroral structure a polar orbiting satellite is most likely to encounter) has to be studied further to see if the proposed relation holds for all longitudes. If this is the case the suggestion that the peaks are superimposed on the smooth region implies that the narrow auroral arcs are produced by a mechanism which is different from that producing the smooth region precipitation.

Acknowledgments

This work was performed while the author was an European Space Research Organization Associate in the Magnetic and Electric Fields Branch at NASA-Goddard Space Flight Center, Greenbelt, Maryland. I am grateful to Dr. R. A. Hoffman for providing access to the OGO-4 data and for many helpful discussions; and to Mrs. Millie Hazard for assistance in preparing the manuscript.

References

Arnoldy, R. L., and K. W. Chan, Particle substorms observed at the geostationary orbit, J. Geophys. Res. 74, 5019-5028, 1969.

Berko, F. W., Distributions and characteristics of high-latitude field-aligned electron precipitation, GSFC Report-X-646-72-190, submitted to J. Geophys. Res, 1972.

Chase, L. M., Evidence that the plasma sheet is the source of auroral electrons, J. Geophys. Res., 74, 348-350, 1969.

DeForest, S. E., and C. E. McIlwain, Plasma clouds in the magnetosphere, J. Geophys. Res., 76, 3587-3611, 1971.

Eather, R. H., and S. B. Mende, Systematics in auroral energy spectra, J. Geophys. Res., 77, 660-673, 1972.

Fairfield, D. H., Average magnetic field configuration of the outer magnetosphere, J. Geophys. Res., 73, 7329-7338, 1968.

Feldstein, Y. I., and G. V. Starkov, Dynamics of auroral belt and polar geomagnetic disturbances, Planet. Space Sci., 15, 209-229, 1967.

Frank, L. A., Initial observations of low energy electrons in the earths magnetosphere with OGO-3, J. Geophys. Res., 72, 185-195, 1967.

Gustafsson, G., Y. I. Feldstein, and N. F. Shevnina, The auroral orientation curves for the IQSY, Planet. Space Sci., 17, 1657-1666, 1969.

Gustafsson, G., Auroral luminosity patterns over Northern Scandinavia, Physica Norvegica 4, 113-119, 1970.

Heppner, J. P., Electric field variations during substorms: OGO-6 measurements, GSFC Report X-645-72-10, 1972.

Hoffman, R. A., and D. S. Evans, OGO-4 auroral particles experiment and calibration, GSFC Report X-611-67-632, 1967.

Hoffman, R. A., and L. S. Evans, Field aligned electron bursts at high latitudes observed by OGO-4, J. Geophys. Res., 73, 6201-6214, 1968.

Hoffman, R. A., and F. W. Berko, Primary electron influx to dayside auroral oval, J. Geophys. Res., 76, 2967-2976, 1971.

Hoffman, R. A., Properties of low energy particle impacts in the polar domain in the dawn and dayside hours, Magnetosphere-Ionosphere Interactions, ed. by K. Folkestad, Universitetsforlaget, Oslo, 1972.

Holmgren, L.-Å., and B. Aparicio, Field aligned electron anisotropies observed by the ESRO1A (Aurorae) satellite, reported at COSPAR, Madrid, 1972.

Hones, E. W., Jr., J. R. Asbridge, S. J. Bame and S. Singer, Energy spectra and angular distributions of particles in the plasma sheet and their comparison with rocket measurements over the auroral zone, J. Geophys. Res., 76, 63-87, 1971.

Hultquist, B., Auroral particles, Geofysiske Publ., 29, 27-55, 1972.

Lezniak, T. W., and J. R. Winckler, Experimental study of magnetospheric motions and the acceleration of energetic electrons during substorms, J. Geophys. Res., 75, 7075-7098, 1970.

Nakada, M. P., J. W. Dungey and W. N. Hess, On the origin of outer-belt protons, J. Geophys. Res., 70, 3529-3532, 1965.

Paulikas, G. A., The patterns and sources of high latitude particle precipitation, Rev. Geophys. and Space Phys., 9, 659, 1971.

Pfitzer, K. A., and J. R. Winckler, Intensity correlations and substorm electron drift effects in the outer radiation belt measured with OGO-3 and ATS-1 satellites, J. Geophys. Res., 74, 5005-5018, 1969.

Riedler, W., and H. Borg, Precipitation patterns of keV electrons and protons, presented at COSPAR General Assembly in Seattle, May, 1971.

Roederer, J. G., On the adiabatic motion of energetic particles in a model magnetosphere, J. Geophys. Res., 72, 981-992, 1967.

Starkov, G. V., Auroral heights in the polar cap, Geomagn. Aeron., 8, 36-41, 1968.

Starkov, G. V., Analytical representation of the equatorial boundary of the auroral zone, Geomagn. Aeron. 9, 759, 1969.

Figure Captions

Figure 1: a-d The location of maximum precipitation as a function of magnetic local time and invariant latitude. The line represents a least square fit and the squares are median values over 3 hours.

Figure 2: The average location of the precipitation for all the energy channels together with the contours of constant magnetic field projected down from the equatorial plane to the height of the satellite.

Figure 3: The location of maximum precipitation of the energies 24, 2.3 and 0.7 keV relative to the location of 7.3 keV precipitation. The line represents the 7.3 keV location.

Figure 4: The variation in latitude of the locus of 7.3 keV precipitation with magnetic activity index Kp.

Figure 5: The differential number flux of electrons as a function of local time. The minimum 0.7 keV level has been defined in the text.

Figure 6: The energy flux spectrum as a function of local time. The broken lines refer to the minimum 0.7 keV level.

Figure 7: An example of a satellite pass demonstrating that the maximum of precipitation for different energies is closer to the equator for higher energies.

Figure 8: The vertical bars show the time delay between the beginning and end of a magnetic bay at midnight and the satellite pass. The abscissa shows the magnetic local time when the satellite passed the maximum precipitation. The width of the bars is related to the intensity of the 2.3 keV precipitation.

Figure 9: From the measured spectrum at satellite altitude in the midnight region a spectrum of the particles in the tail has been estimated. Four spectra obtained by the Vela satellites have been included for comparison.

Figure 10: a-b Two examples of particle precipitation during satellite passes in the dawn region. The examples demonstrate the shift in latitude for different energies and the peaked poleward precipitation of 0.7 keV.

Figure 11: a-b Examples of particle precipitation during midnight passes. Orbit 888 shows 0.7 keV peaked precipitation superimposed on the 7.3 keV region down to 66.4° invariant latitude, in orbit 2606 the regions are separated.

Figure 12: The region of peaked 0.7 keV precipitation as a function of magnetic local time and latitude. The line shows the auroral orientation curve crossing the midnight meridian at 68° invariant latitude. In the midnight sector only peaks to the poleward side of the main 7.3 keV precipitation has been included.

Figure 13: The amplitude of the largest 0.7 keV peak for each satellite pass as a function of magnetic local time.

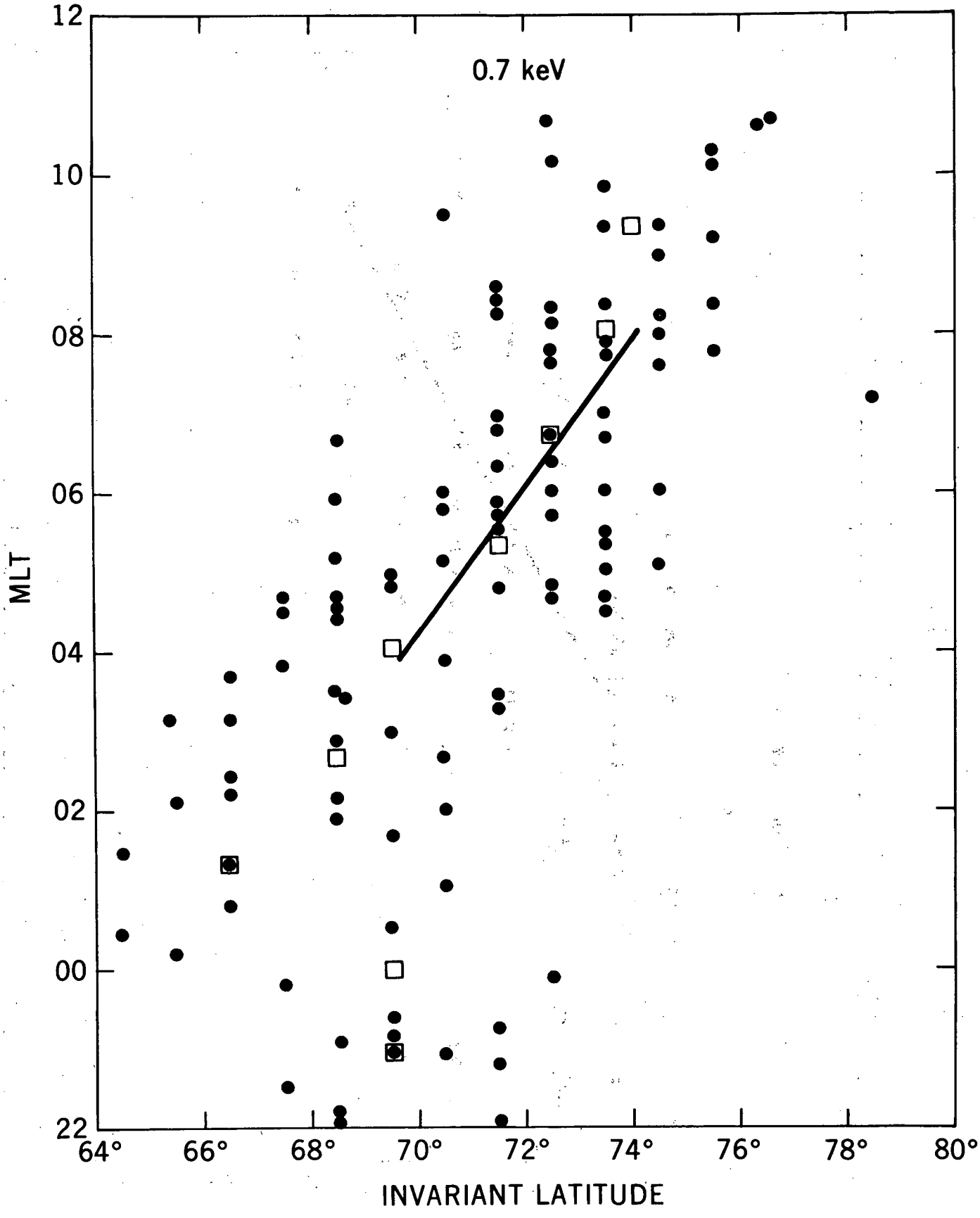
0.7 keV
12
10
08
06
04
02
00
22
MLT
64°
66°
68°
70°
72°
74°
76°
78°
80°
INVARIANT LATITUDE

FIGURE 1a

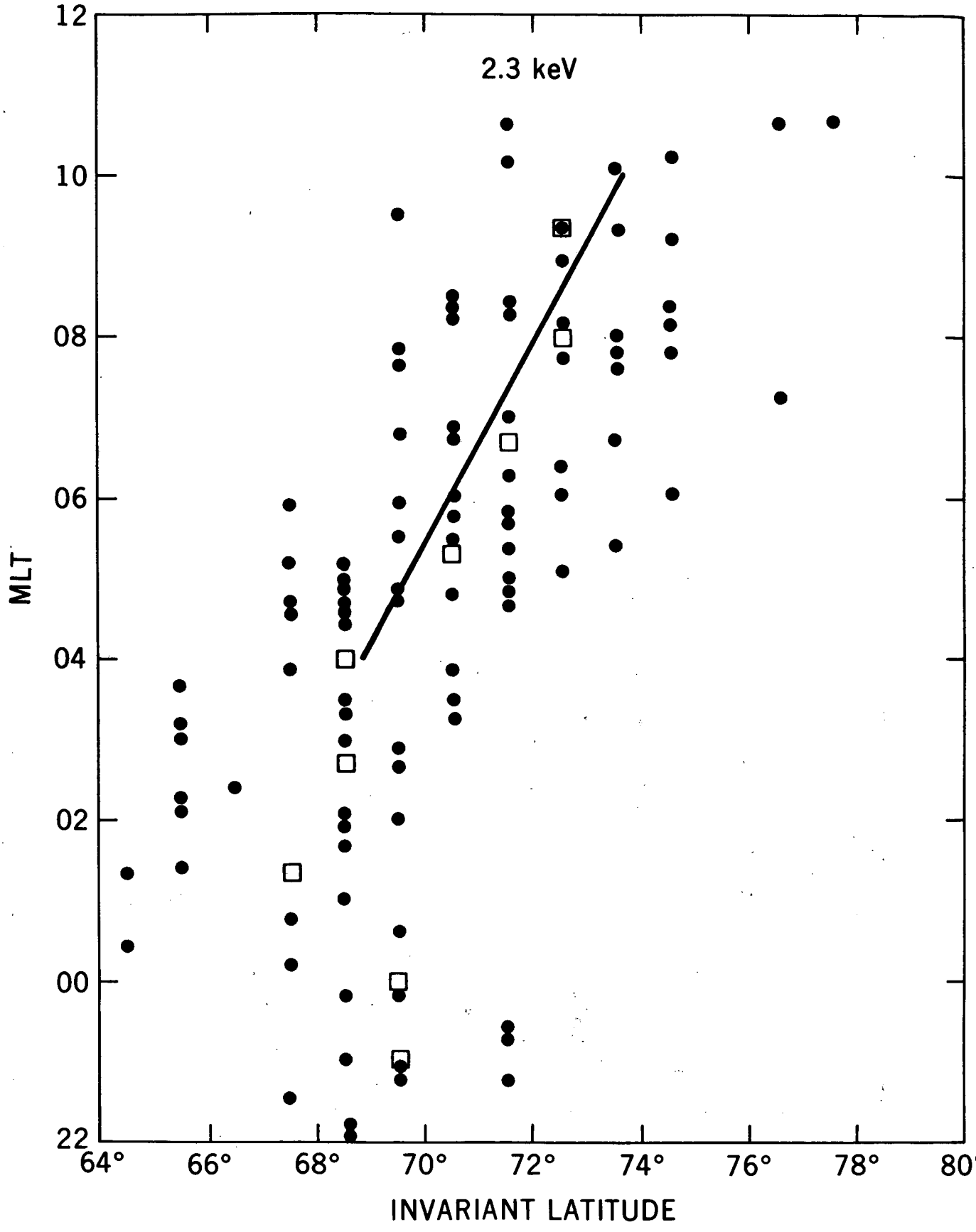
2.3 keV
12
10
08
06
04
02
00
22
MLT
64°
66°
68°
70°
72°
74°
76°
78°
80°
INVARIANT LATITUDE

FIGURE 1b

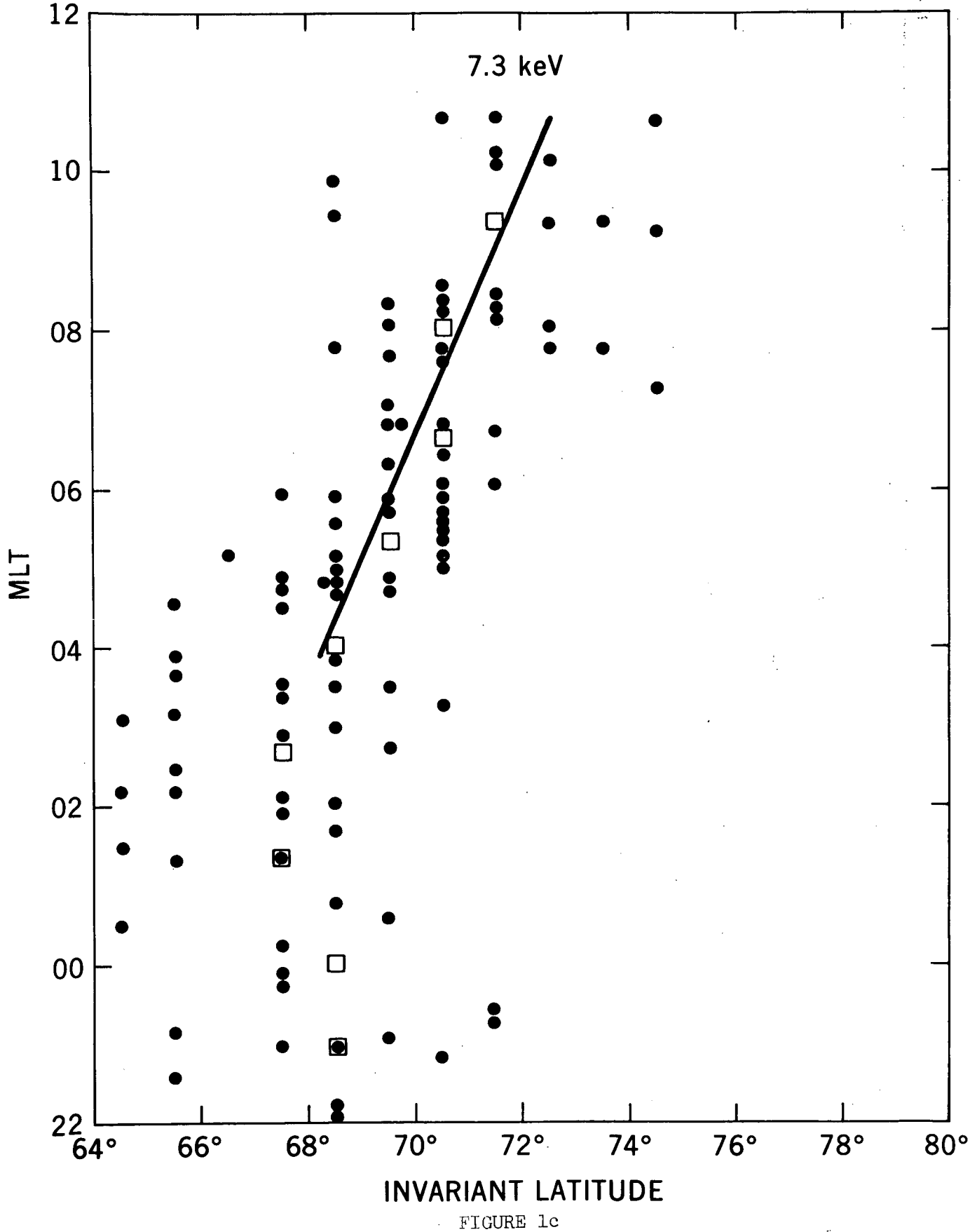
7.3 keV
12
10
08
06
04
02
00
22
MLT
64°
66°
68°
70°
72°
74°
76°
78°
80°
INVARIANT LATITUDE

FIGURE 1c

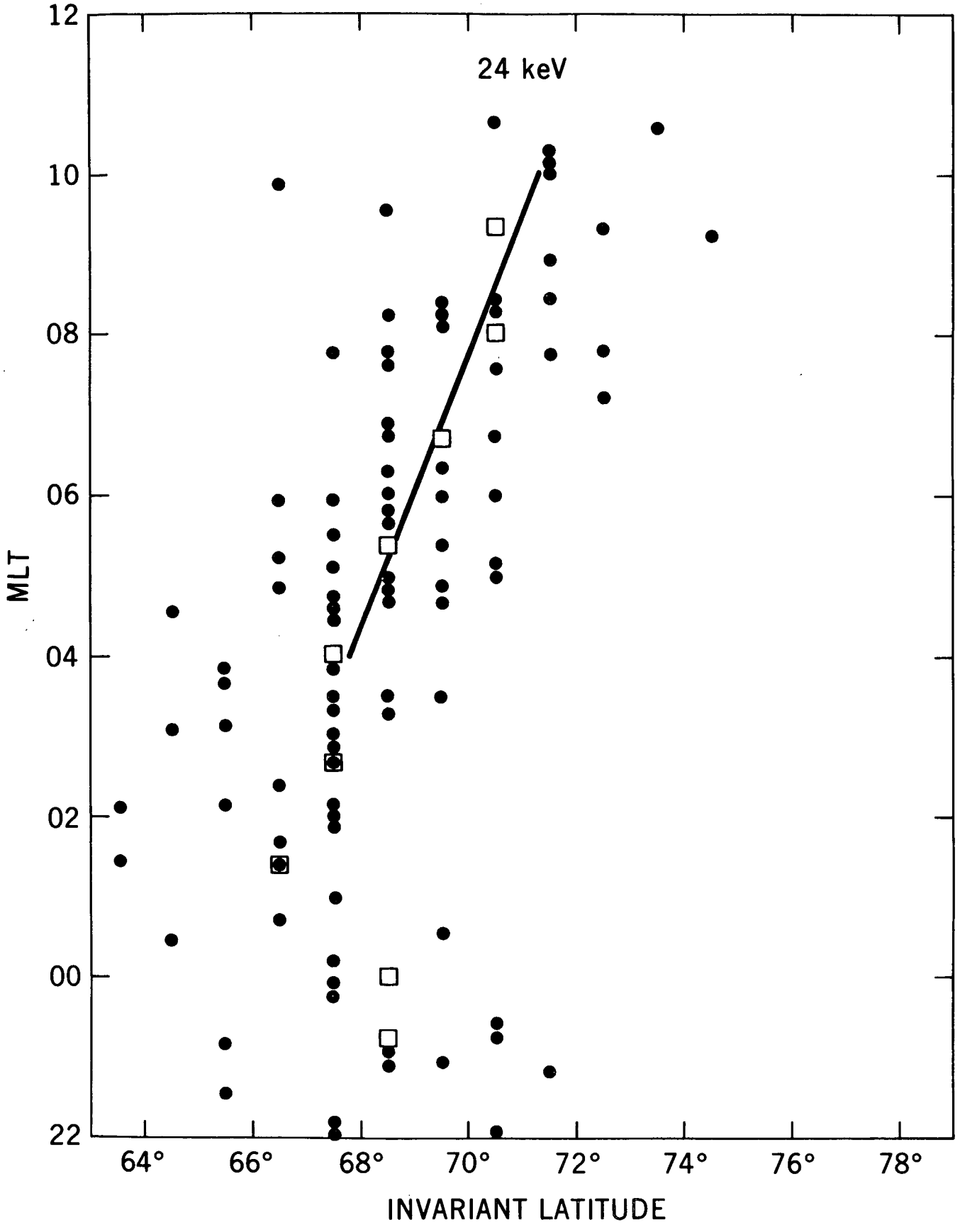
24 keV
12
10
08
06
04
02
00
22
MLT
64°
66°
68°
70°
72°
74°
76°
78°
INVARIANT LATITUDE

FIGURE 1d

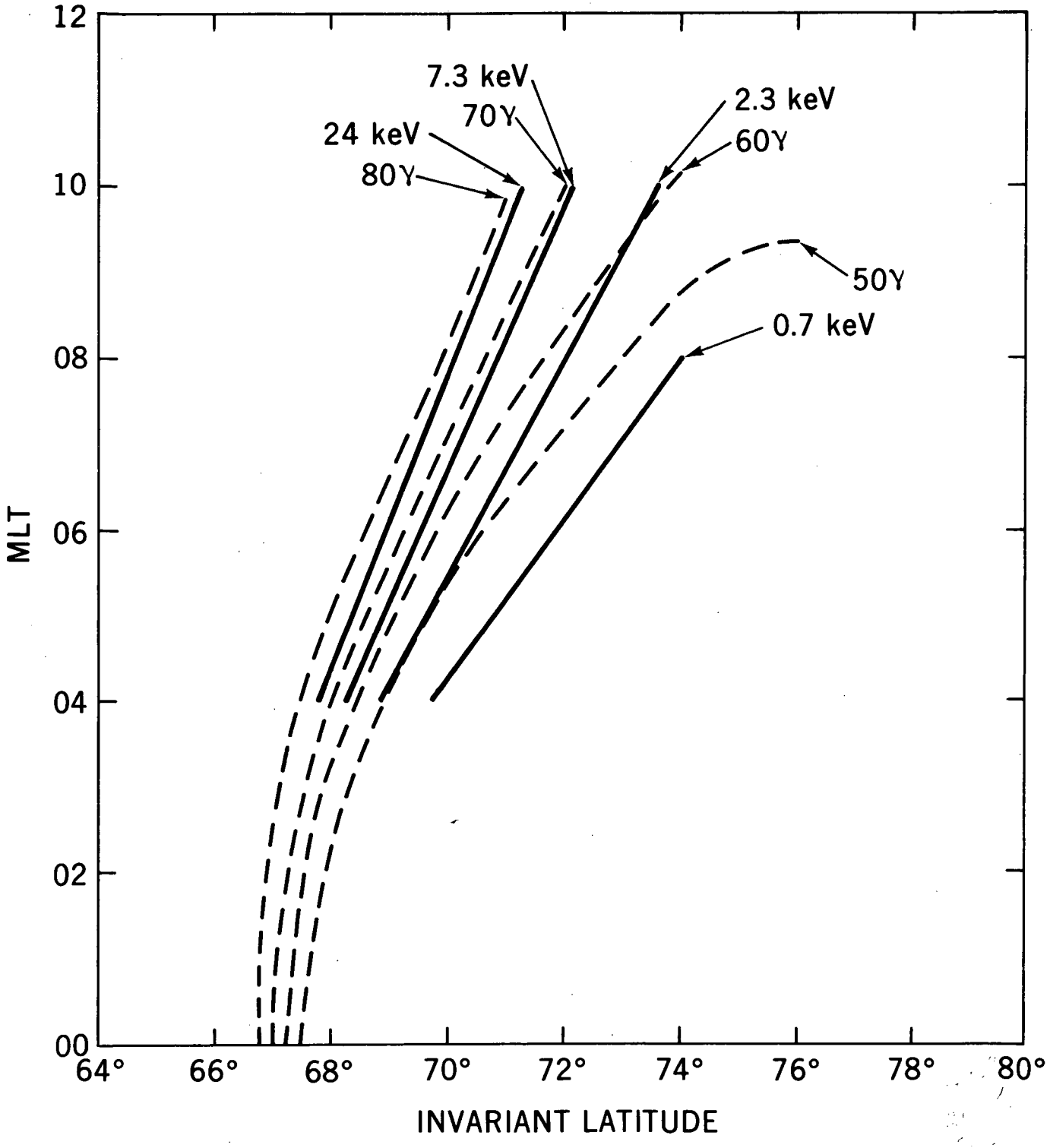
12
10
08
06
04
02
00
MLT
64°
66°
68°
70°
72°
74°
76°
78°
80°
INVARIANT LATITUDE
7.3 keV
70γ
24 keV
80γ
2.3 keV
60γ
50γ
0.7 keV

FIGURE 2

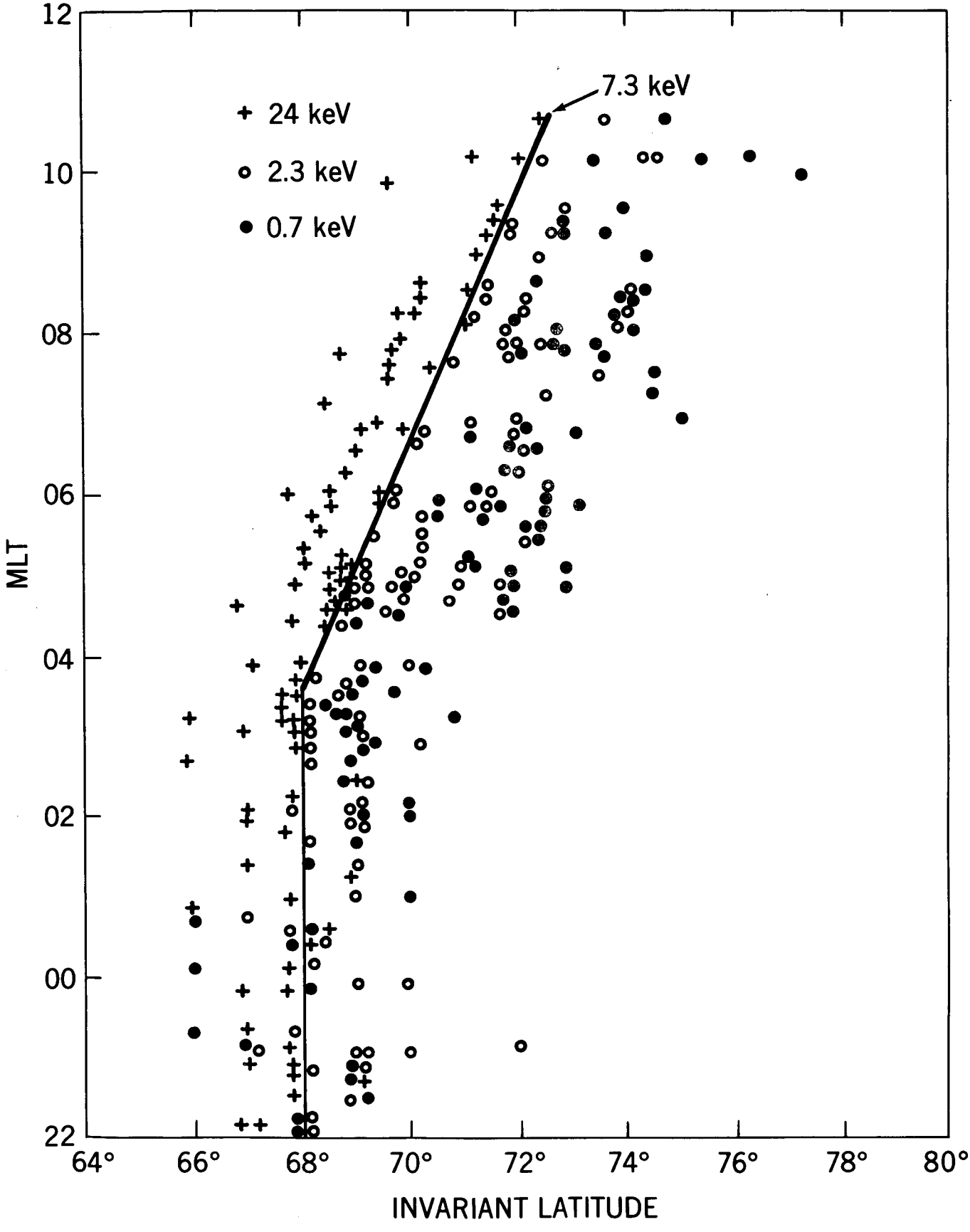
12
10
08
06
04
02
00
22
MLT
64°
66°
68°
70°
72°
74°
76°
78°
80°
INVARIANT LATITUDE
24 keV
2.3 keV
0.7 keV
7.3 keV

FIGURE 3

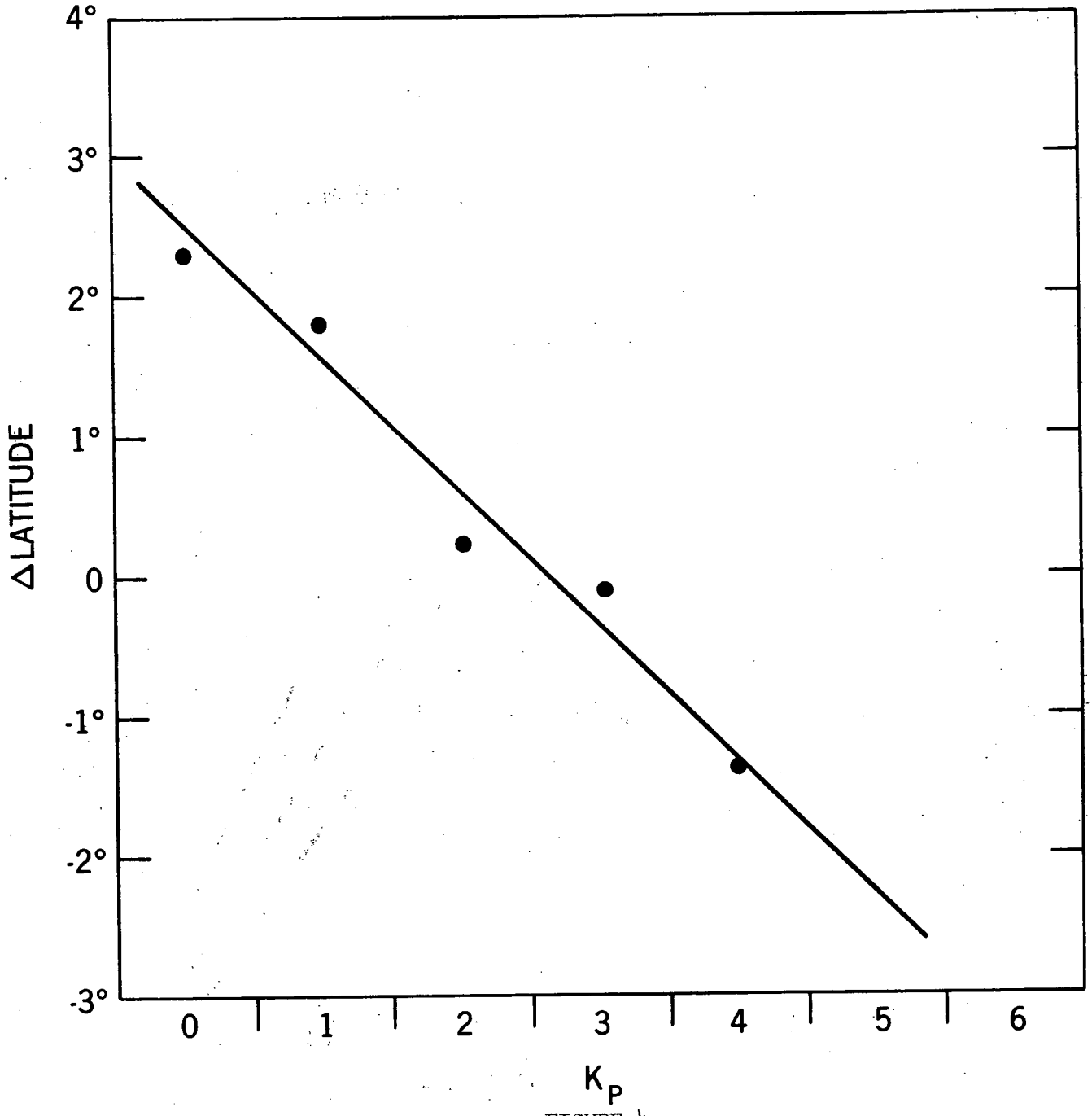

FIGURE 4

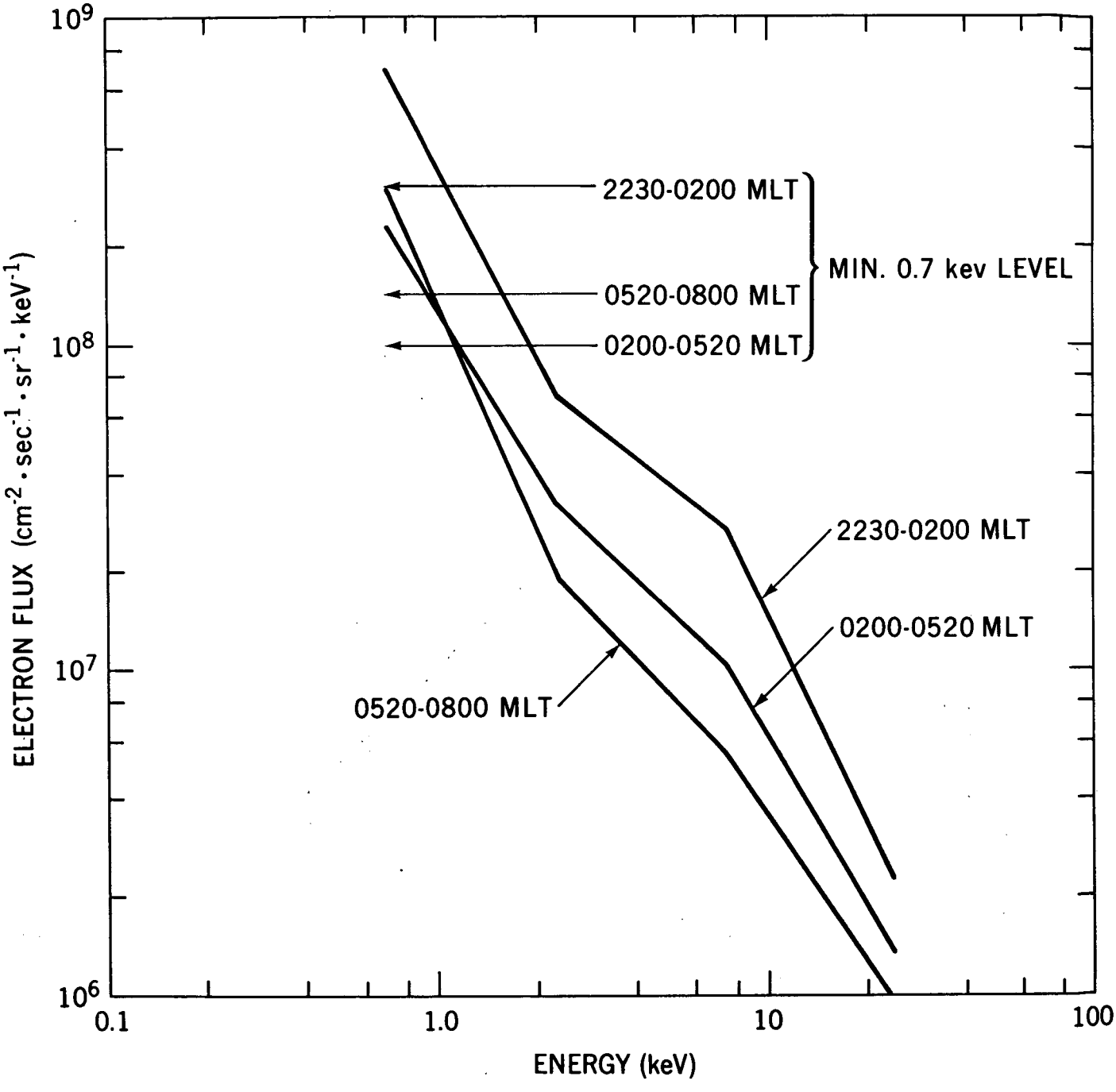
10^9
10^8
10^7
10^6
ELECTRON FLUX ($cm^{-2} \cdot sec^{-1} \cdot sr^{-1} \cdot keV^{-1}$)
2230-0200 MLT
0520-0800 MLT
0200-0520 MLT
MIN. 0.7 kev LEVEL
2230-0200 MLT
0200-0520 MLT
0520-0800 MLT
0.1
1.0
10
100
ENERGY (keV)

FIGURE 5

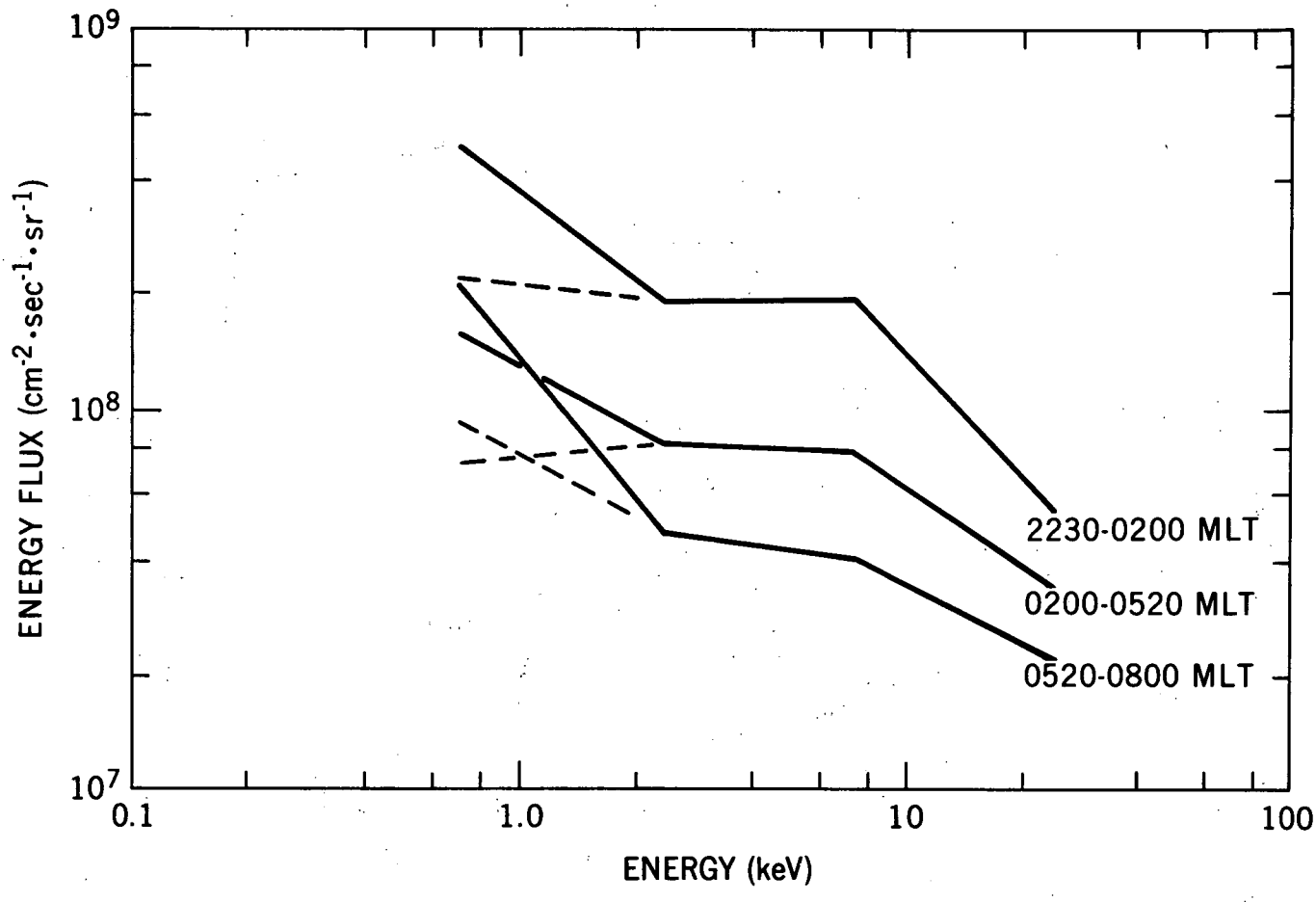
10^9
10^8
10^7
ENERGY FLUX ($cm^{-2} \cdot sec^{-1} \cdot sr^{-1}$)
0.1
1.0
10
100
ENERGY (keV)
2230-0200 MLT
0200-0520 MLT
0520-0800 MLT

FIGURE 6

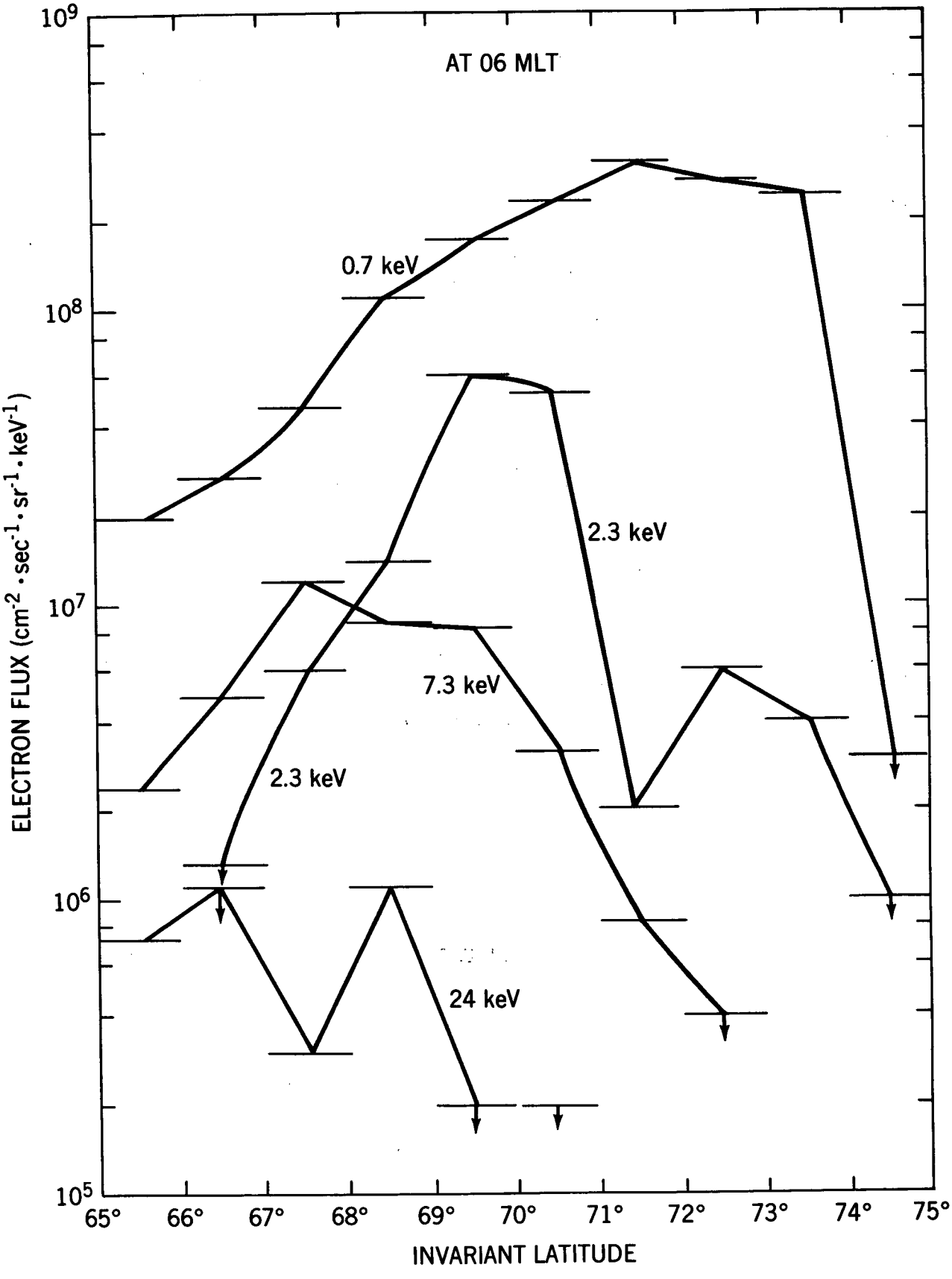
AT 06 MLT
0.7 keV
2.3 keV
7.3 keV
2.3 keV
24 keV
10^9
10^8
10^7
10^6
10^5
ELECTRON FLUX ($cm^{-2} \cdot sec^{-1} \cdot sr^{-1} \cdot keV^{-1}$)
65°
66°
67°
68°
69°
70°
71°
72°
73°
74°
75°
INVARIANT LATITUDE

FIGURE 7

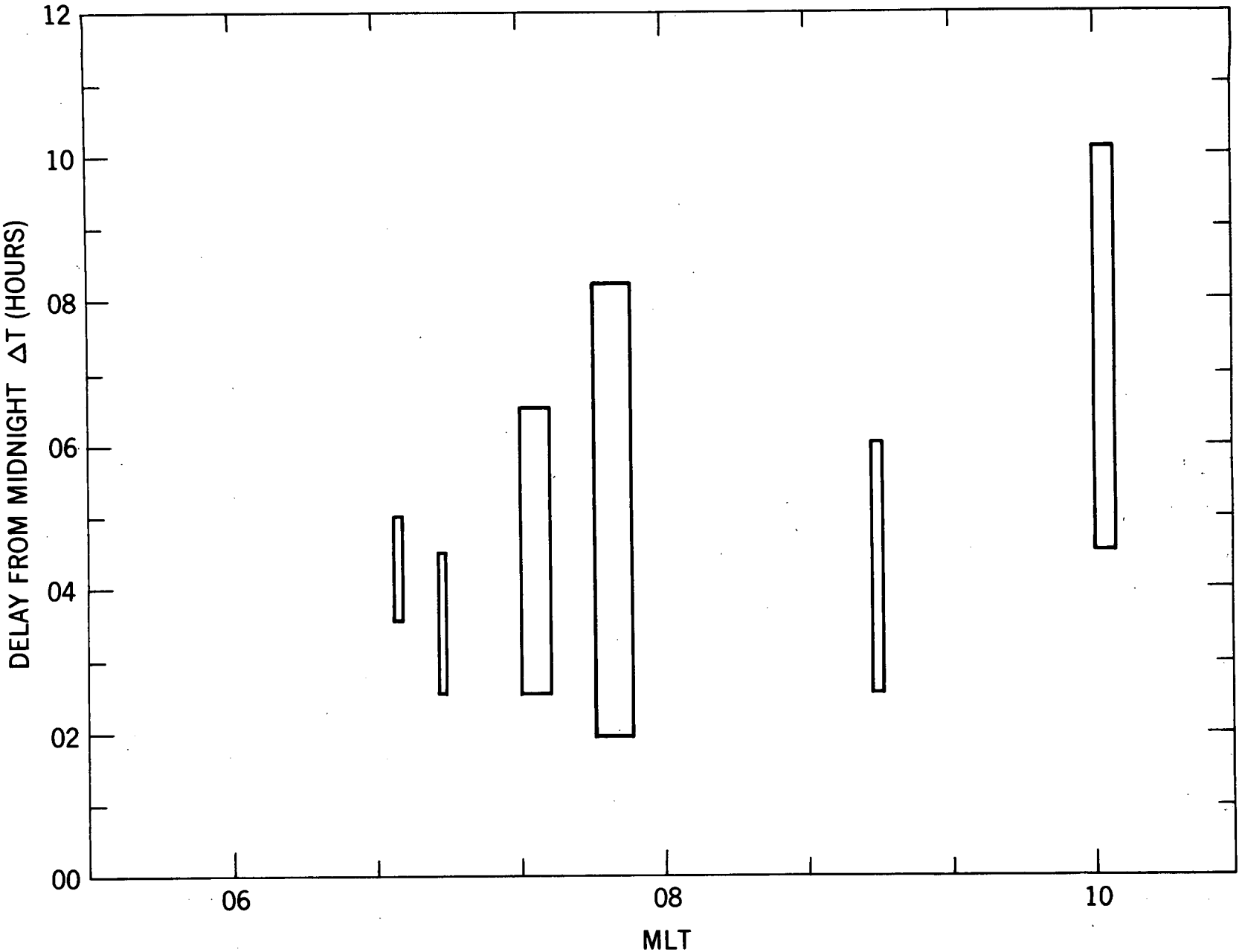

FIGURE 8

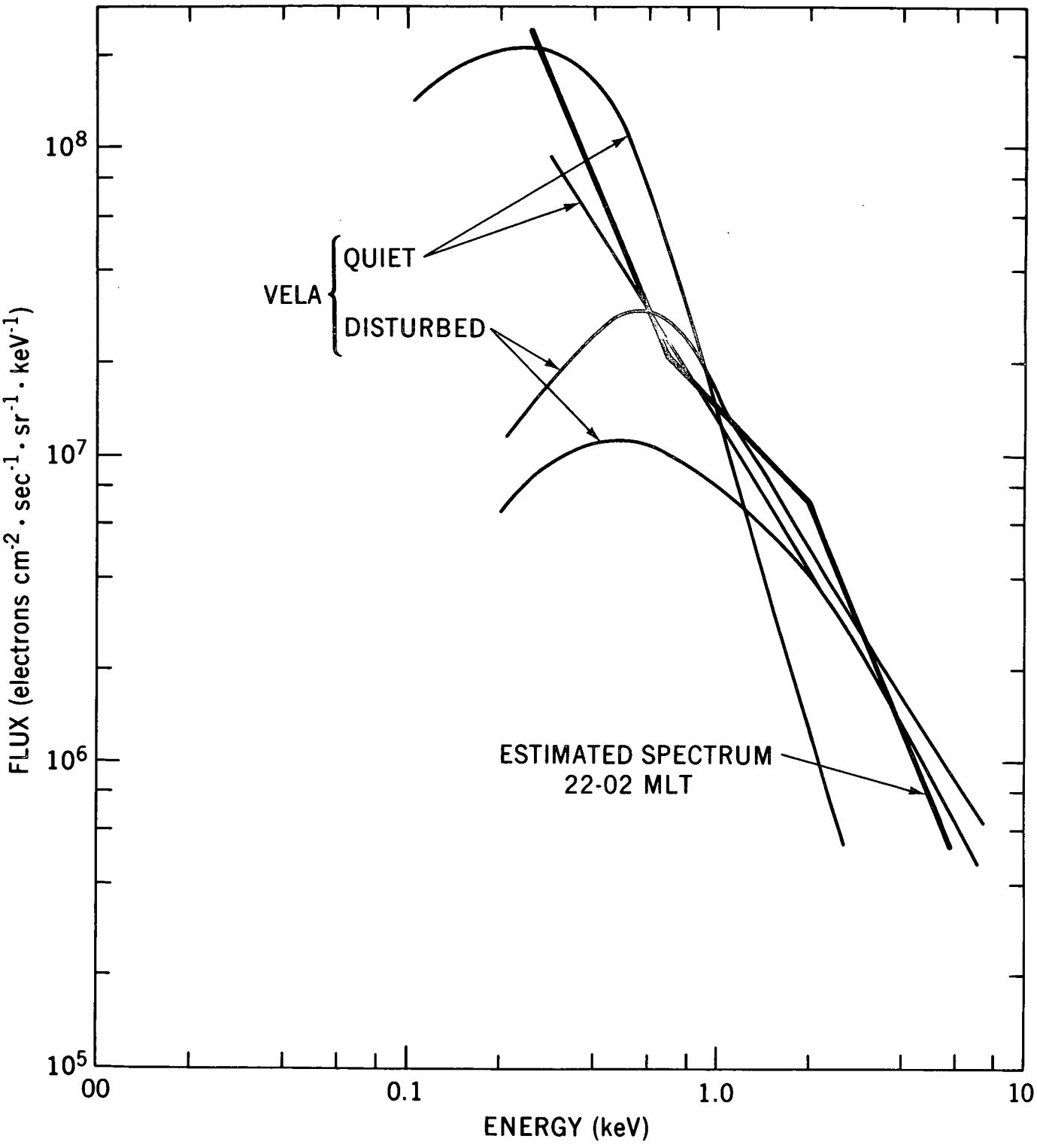
10^8
10^7
10^6
10^5
FLUX (electrons $cm^{-2} \cdot sec^{-1} \cdot sr^{-1} \cdot keV^{-1}$)
VELA
QUIET
DISTURBED
ESTIMATED SPECTRUM
22-02 MLT
00
0.1
1.0
10
ENERGY (keV)

FIGURE 9

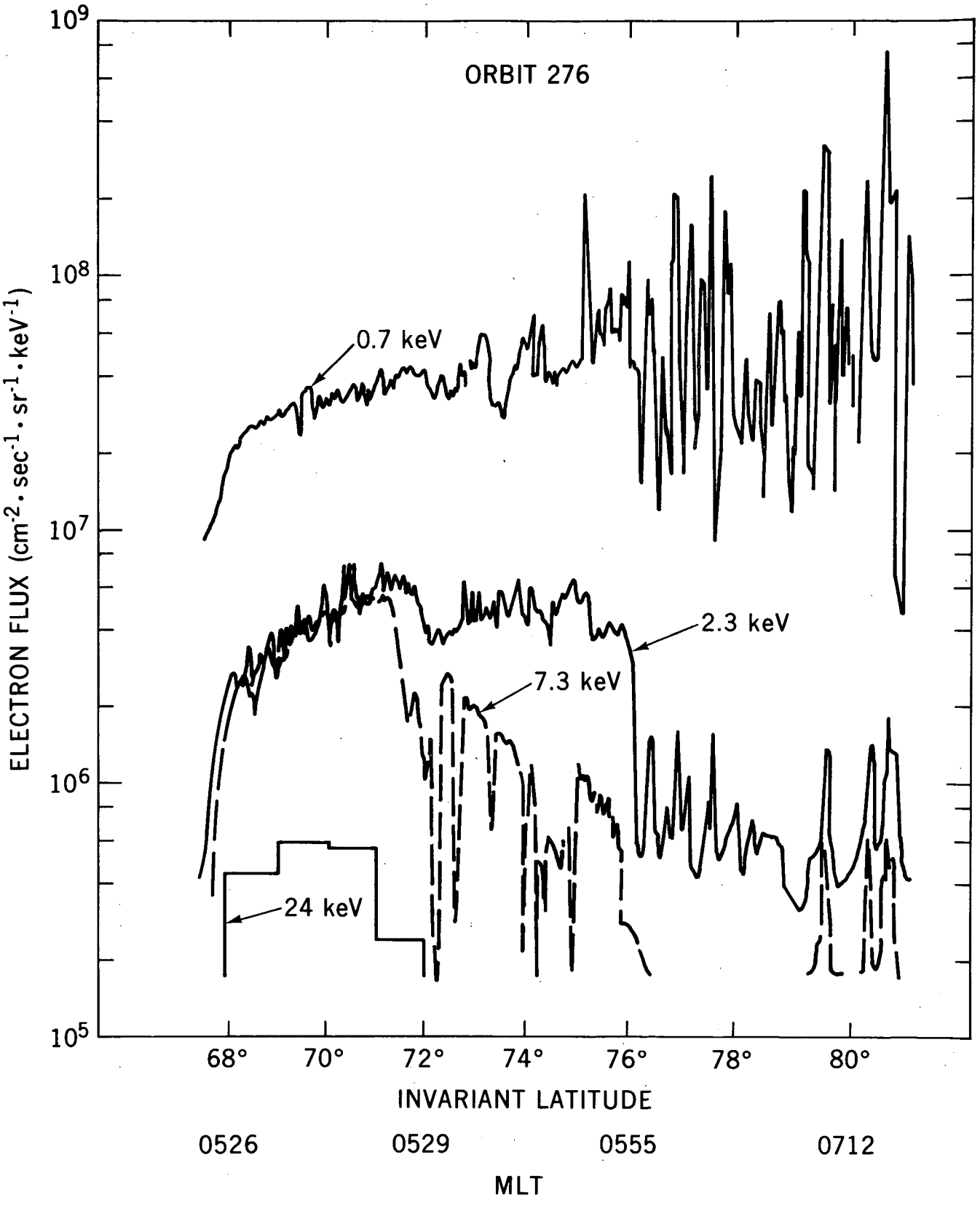
ORBIT 276
ELECTRON FLUX (cm^{-2} · sec^{-1} · sr^{-1} · keV^{-1})
10^9
10^8
10^7
10^6
10^5
0.7 keV
2.3 keV
7.3 keV
24 keV
68°
70°
72°
74°
76°
78°
80°
INVARIANT LATITUDE
0526
0529
0555
0712
MLT

FIGURE 10a

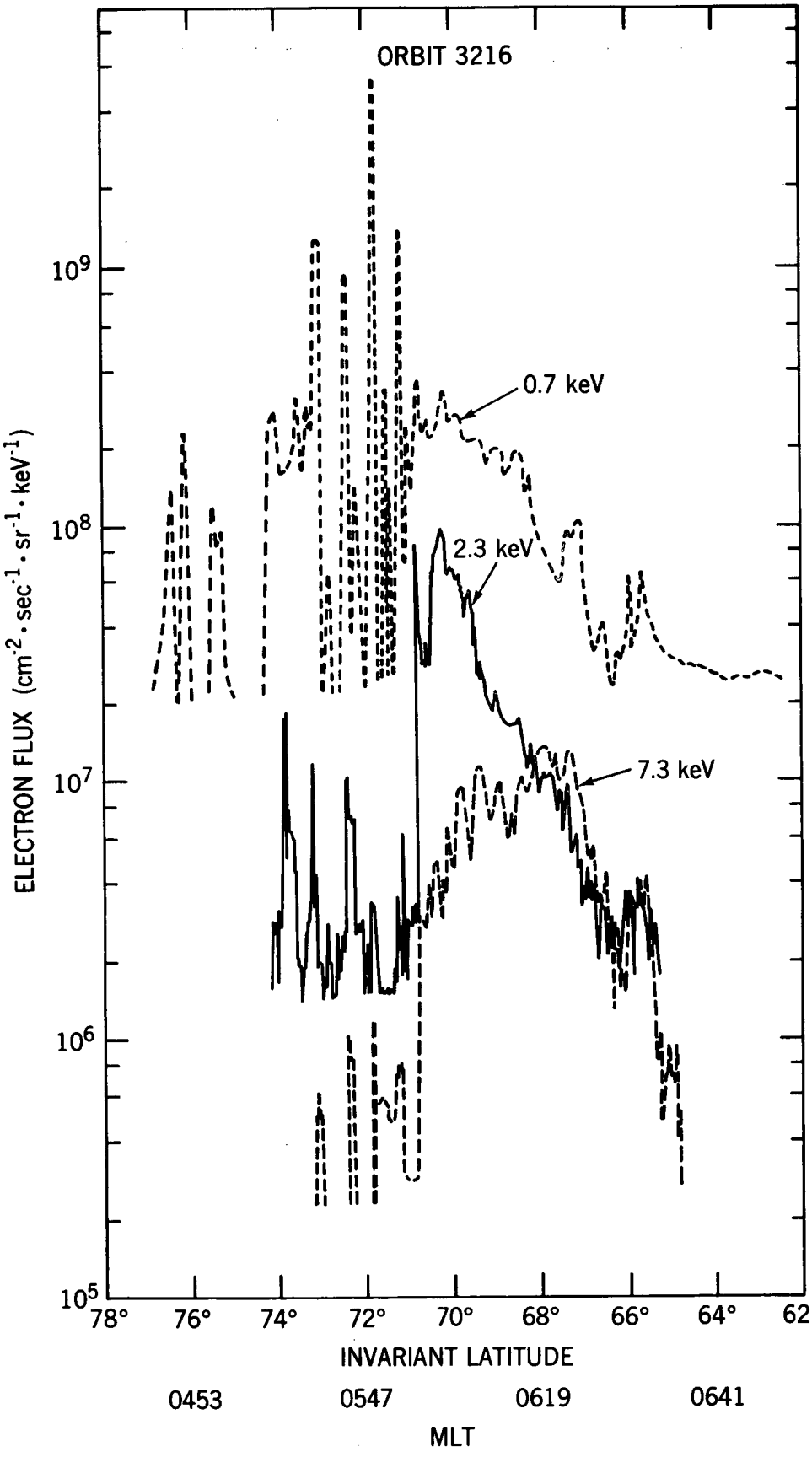
ORBIT 3216
0.7 keV
2.3 keV
7.3 keV
ELECTRON FLUX (cm^{-2} · sec^{-1} · sr^{-1} · keV^{-1})
10^9
10^8
10^7
10^6
10^5
78°
76°
74°
72°
70°
68°
66°
64°
62°
INVARIANT LATITUDE
0453
0547
0619
0641
MLT

FIGURE 10b

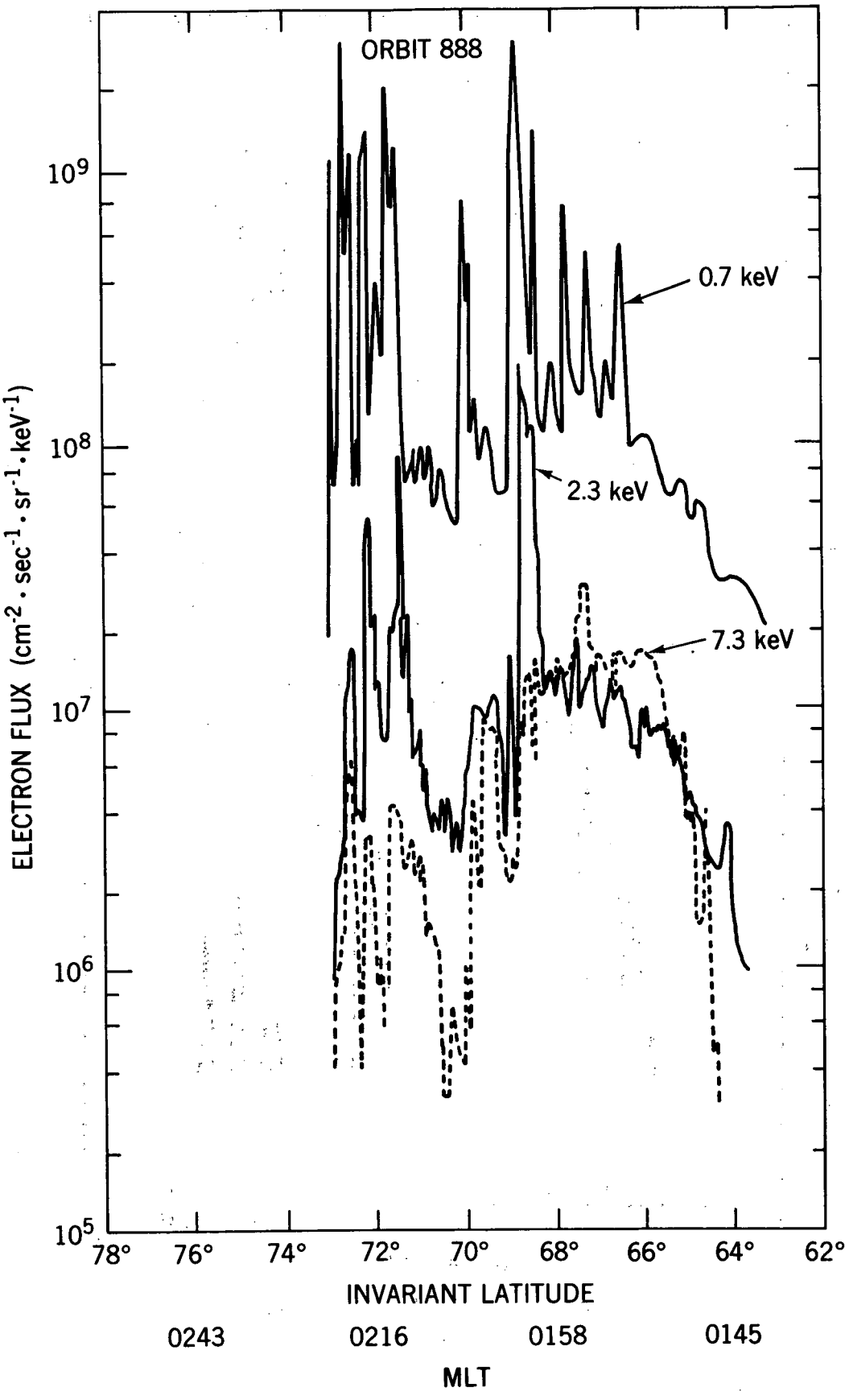
ORBIT 888
0.7 keV
2.3 keV
7.3 keV
ELECTRON FLUX (cm^{-2} · sec^{-1} · sr^{-1} · keV^{-1})
10^9
10^8
10^7
10^6
10^5
78°
76°
74°
72°
70°
68°
66°
64°
62°
INVARIANT LATITUDE
0243
0216
0158
0145
MLT

FIGURE 11a

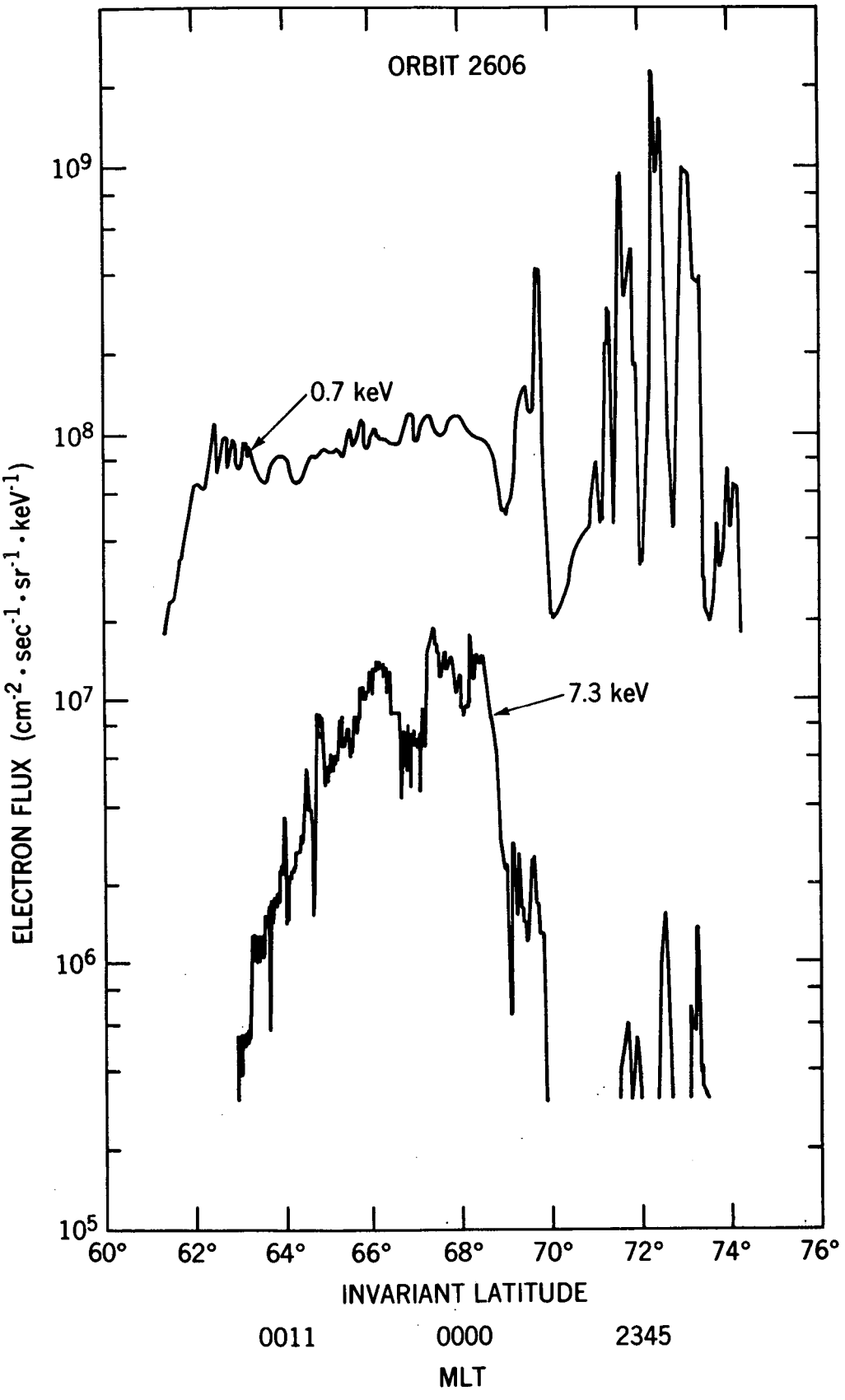
ORBIT 2606
0.7 keV
7.3 keV
ELECTRON FLUX (cm^{-2} · sec^{-1} · sr^{-1} · keV^{-1})
10^9
10^8
10^7
10^6
10^5
60°
62°
64°
66°
68°
70°
72°
74°
76°
INVARIANT LATITUDE
0011
0000
2345
MLT

FIGURE 11b

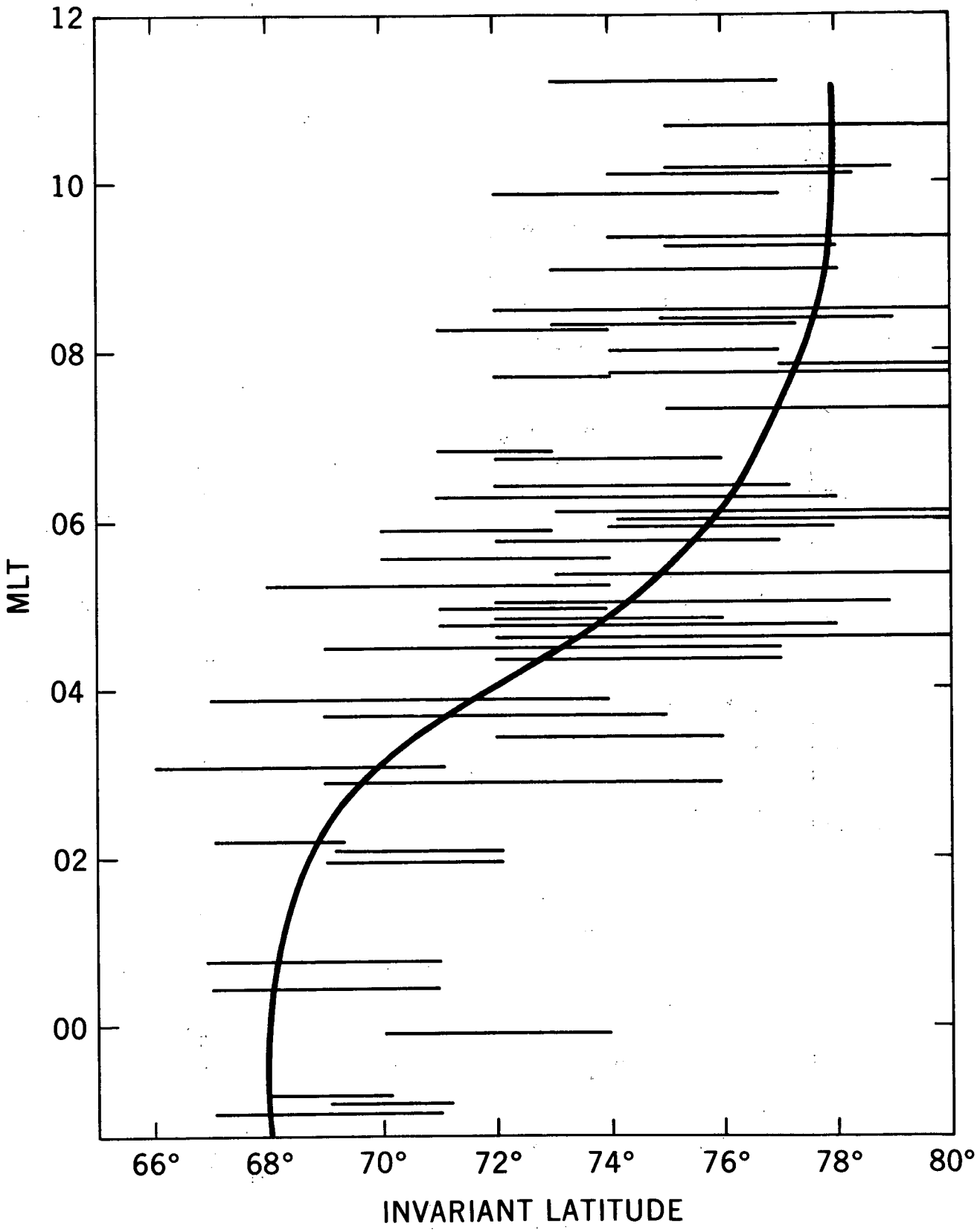
12
10
08
06
04
02
00
MLT
66°
68°
70°
72°
74°
76°
78°
80°
INVARIANT LATITUDE

FIGURE 12

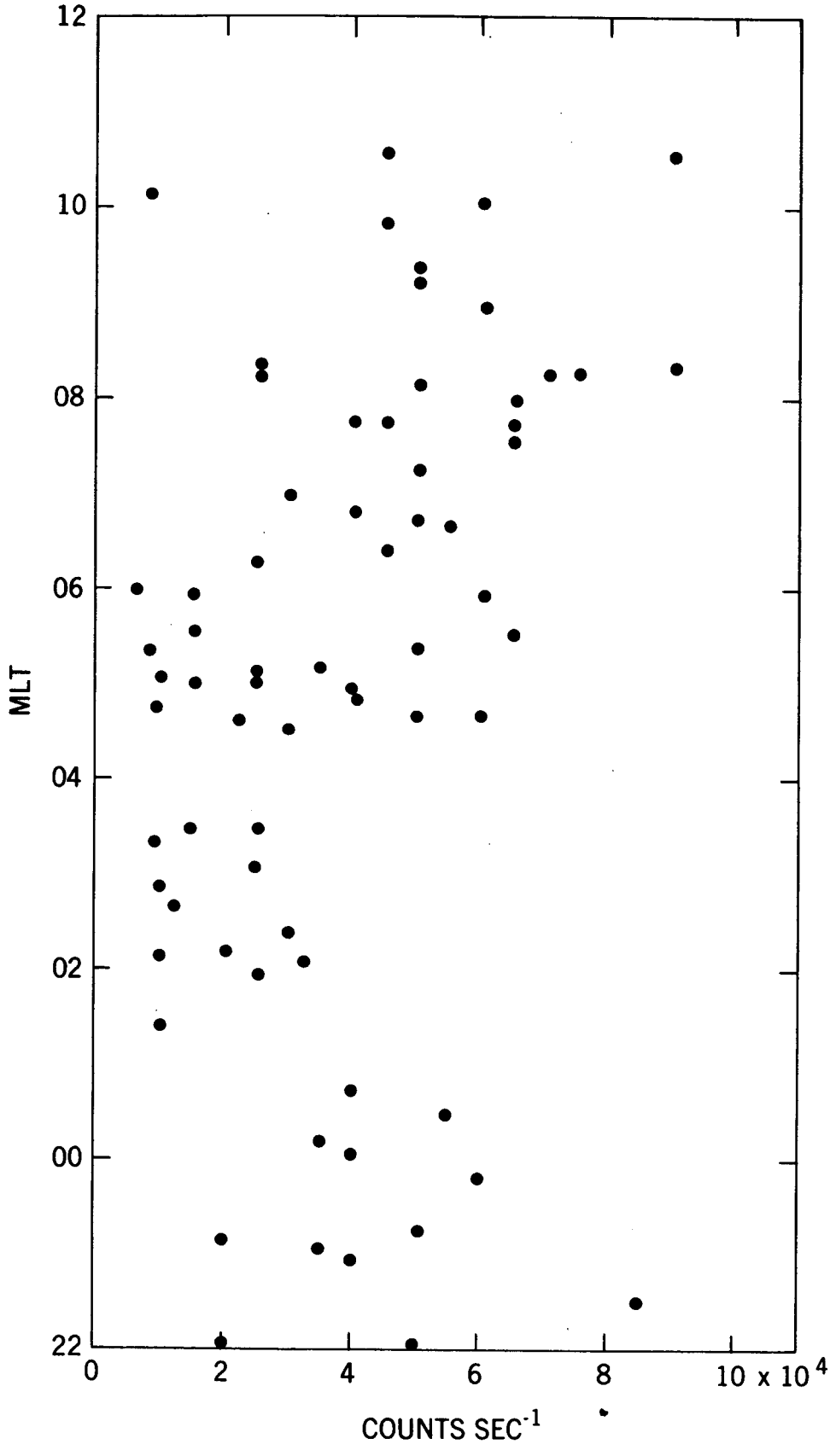

FIGURE 13